








## METHODS AND RESOURCES

# Optimizing electrical field stimulation parameters reveals the maximum contractile function of human skeletal muscle microtissues

Yekaterina Tiper,<sup>1,2</sup> Zhuoye Xie,<sup>1,2</sup>  Arne Hofemeier,<sup>3,4</sup> Heta Lad,<sup>1,2</sup>  Mattias Luber,<sup>5</sup>  Roman Krawetz,<sup>6,7</sup>  Timo Betz,<sup>5,8</sup> Wolfram-Hubertus Zimmermann,<sup>3,4,8,9,10,11</sup>  Aaron B. Morton,<sup>12,13</sup>  Steven S. Segal,<sup>12,14,15,16,17</sup> and  Penney M. Gilbert<sup>1,2,18</sup>

<sup>1</sup>Institute of Biomedical Engineering, University of Toronto, Toronto, Ontario, Canada; <sup>2</sup>Donnelly Centre, University of Toronto, Toronto, Ontario, Canada; <sup>3</sup>Institute of Pharmacology and Toxicology, University Medical Center Göttingen, Göttingen, Germany; <sup>4</sup>German Center for Cardiovascular Research (DZHK), Partner site Lower Saxony, Göttingen, Germany; <sup>5</sup>Third Institute of Physics, University of Göttingen, Göttingen, Germany; <sup>6</sup>Department of Cell Biology and Anatomy, University of Calgary, Calgary, Alberta, Canada; <sup>7</sup>Cummings School of Medicine, University of Calgary, Calgary, Alberta, Canada; <sup>8</sup>Cluster of Excellence "Multiscale Bioimaging: from Molecular Machines to Networks of Excitable Cells", University of Göttingen, Göttingen, Germany; <sup>9</sup>German Center for Neurodegenerative Diseases (DZNE), Göttingen, Germany; <sup>10</sup>German Center for Child and Adolescent Health (DZKJ), Göttingen, Germany; <sup>11</sup>Fraunhofer Institute for Translational Medicine and Pharmacology, Göttingen, Germany; <sup>12</sup>Department of Medical Pharmacology and Physiology, University of Missouri School of Medicine, Columbia, Missouri, United States; <sup>13</sup>Department of Kinesiology and Sport Management, Texas A&M University, College Station, Texas, United States; <sup>14</sup>Dalton Cardiovascular Research Center, University of Missouri, Columbia, Missouri, United States; <sup>15</sup>Department of Biomedical Sciences, University of Missouri, Columbia, Missouri, United States; <sup>16</sup>Department of Biomedical, Biological and Chemical Engineering, University of Missouri, Columbia, Missouri, United States; <sup>17</sup>Department of Nutrition and Exercise Physiology, University of Missouri, Columbia, Missouri, United States; and <sup>18</sup>Department of Cell and Systems Biology, University of Toronto, Toronto, Ontario, Canada

## Abstract

Skeletal muscle microtissues are engineered to develop therapies for restoring muscle function in patients. However, optimal electrical field stimulation (EFS) parameters to evaluate the function of muscle microtissues remain unestablished. This study reports a protocol to optimize EFS parameters for eliciting contractile force of muscle microtissues cultured in micropost platforms. Muscle microtissues were produced across an opposing pair of microposts in polydimethylsiloxane and polymethyl methacrylate culture platforms using primary, immortalized, and induced pluripotent stem cell-derived myoblasts. In response to EFS between needle electrodes, contraction deflects microposts proportional to developed force. At 5 V, pulse durations used for native muscle (0.1–1 ms) failed to elicit contraction of microtissues; durations reported for engineered muscle (5–10 ms) failed to elicit peak force. Instead, pulse durations of 20–80 ms were required to elicit peak twitch force across microtissues derived from five myoblast lines. Similarly, although peak tetanic force occurs at 20–50 Hz for native human muscles, it varied across microtissues depending on the cell line type, ranging from 7 to 60 Hz. A new parameter, the dynamic oscillation of force, captured trends during rhythmic contractions, whereas quantifying the duration-at-peak force provides an extended kinetics parameter. Our findings indicate that muscle microtissues have cell line type-specific contractile properties, yet all contract and relax more slowly than native muscle, implicating underdeveloped excitation-contraction coupling. Failure to optimize EFS parameters can mask the functional potential of muscle microtissues by underestimating force production. Optimizing and reporting EFS parameters and metrics is necessary to leverage muscle microtissues for advancing skeletal muscle therapies.

**NEW & NOTEWORTHY** Electrical field stimulation (EFS) parameters remain to be standardized for engineered skeletal muscle. Herein, we report a protocol for defining EFS parameters that elicit the maximal contractile force of muscle microtissues cultivated in micropost devices and highlight the value of developing appropriate metrics. The dynamic oscillation of force and duration-at-peak force are introduced as novel metrics of contraction kinetics.

*contractile function; electrical field stimulation; engineered skeletal muscle; induced pluripotent stem cells; micropost platform*



Correspondence: P. M. Gilbert (penney.gilbert@utoronto.ca).  
Submitted 7 May 2024 / Revised 7 June 2024 / Accepted 20 February 2025



## INTRODUCTION

Skeletal muscle, the most abundant tissue in the human body by mass, performs mechanical, metabolic, and endocrine functions (1, 2). Its primary role is to produce contractile force by converting an electrical stimulus to a mechanical response through excitation-contraction coupling (3). The maintenance of skeletal muscle mass and function is essential for mobility and metabolic homeostasis, but these qualities of life are compromised in congenital myopathies and muscular dystrophies (4), disrupted or destroyed with muscle injury (5, 6), and progressively decline during aging (7). To combat such conditions of skeletal muscle dysfunction requires novel strategies and engineered models that accurately evaluate function.

Studies of native muscle *in vivo* and of two-dimensional (2-D) cell cultures *in vitro* have advanced our understanding of skeletal muscle structure, function, and pathology. Nonetheless, animal models are costly, time consuming, and may not fully recapitulate human muscle disease (8, 9). Species-specific differences in drug metabolism also limit the clinical translation of therapeutics (10). In 2-D cell cultures, human myotubes with well-defined sarcomeric development (11, 12) easily detach from the cell culture substratum (13). A promising strategy to overcome these limitations entails the development of three-dimensional (3-D) skeletal muscle microtissues. Although functionally and structurally inferior to native muscle, engineered muscle microtissues are promising models of myopathy (14–16) and drug discovery (17–19) through providing alternatives to animal studies.

Skeletal muscle microtissues have been developed that enable the evaluation of contractile force and the effects of experimental interventions *in vitro* (20). Although no standard platform for evaluating contractile force produced by muscle microtissues has been established, three prevalent techniques have emerged. 1) In cantilever deflection, 2-D cultures of myotubes differentiated on a flexible substrate are fixed at one end and free at the other (15, 21, 22). Myotube contraction produces vertical displacement of the free end of the cantilever that is proportional to the force exerted. 2) With micropost deflection, a pair of vertical microposts serves as anchor points for the culture of microtissues comprised of myotube bundles (17, 23, 24); horizontal displacement of microposts measured optically provides a measure of contractile force. 3) The pin secured technique uses hooks to secure each end of the muscle microtissue with one end connected to a force transducer (18, 19, 25). Although the latter approach is more invasive with lower throughput, its use of a linear actuator enables evaluation of the length-force relationship (18, 25). The present study centers on micropost systems, which enable noninvasive assessment of contractile force of engineered 3-D skeletal muscle microtissues with high throughput.

Electrical field stimulation (EFS) is used to initiate muscle contraction *in vitro* and has been implemented in all three muscle microtissue platforms. Electric current depolarizes the sarcolemma, triggers an action potential, and leads to the release of  $\text{Ca}^{2+}$  from the sarcoplasmic reticulum (SR) to activate the contractile proteins followed by  $\text{Ca}^{2+}$  reuptake and relaxation. A twitch is generated by firing a single action potential whereas a fused tetanus is produced when action

potentials are delivered at sufficient frequency to prevent relaxation of muscle fibers between successive stimuli (26). Although twitch and tetanic forces of muscle microtissues have been reported, few studies have evaluated their contraction and relaxation times and rates to offer a comprehensive analysis of kinetics (20).

A current challenge to address is the variability in force reported across studies of engineered muscle tissue, which is challenging to interpret given the lack of a standardized approach for selecting and reporting electrical stimulation parameters (20). The use of suboptimal stimulation may not only underestimate the force developed by muscle microtissues but can also produce inordinate fatigue and electrochemical damage (27). Such undesirable consequences emphasize the need to optimize the parameters of stimulus voltage, pulse duration, and frequency, so as to accurately assess the functional potential of engineered muscle tissue. To our knowledge, no study has reported optimizing the stimulus parameters for eliciting the peak twitch and tetanic force of skeletal muscle microtissues.

We previously reported MyoTACTIC, a multiwell culture device cast with all features from a polyurethane mold, that enables fabrication of 96 human skeletal muscle microtissues (hMMTs) for investigating contractile force based on micropost deflection (17). The present protocol was designed to systematically evaluate the parameters of EFS to determine the optimal stimulus conditions for peak twitch tension and for peak tetanic contraction of hMMTs engineered from human myoblasts using the MyoTACTIC model. Experiments to demonstrate the generalizability of the approach across protocol users, micropost culture devices, and distinct myoblast cell line types (primary, immortalized, induced pluripotent stem cell derived) are presented. We also report two new parameters: 1) dynamic oscillation of force (DOF), to define the force trends during repetitive contractions and 2) duration-at-peak, which delivers extended kinetics parameters.

## MATERIALS AND METHODS

### MyoTACTIC Culture Platform Fabrication

The polydimethylsiloxane (PDMS) MyoTACTIC 96-well platform used for the culture of 3-D hMMTs was fabricated as described (17, 28). In short, a rigid, reusable polyurethane (PU) negative mold was cast through the sequential fabrication of two flexible PDMS intermediates from the original 3-D printed, 96-well plate design. Smooth-Cast 310 liquid plastic (Smooth-On; Macungie, PA) and Sylgard 184 silicone elastomer (Dow Corning; Midland, MI) were used for the PU and PDMS casting steps, respectively. The PU negative mold then served as a template for the repeated generation of PDMS replicas of the MyoTACTIC plate with all features fabricated in this single casting step. Before use, the 96-well platform was cut into portions that each contained  $6 \pm 2$  wells then autoclaved in an instrument sterilization bag. The culture wells were incubated overnight at 4°C with 100  $\mu\text{L}$  of a Pluronic F-127 (Cat. No. P2443, Sigma; Burlington, MA) solution diluted to 5% in  $\text{dH}_2\text{O}$  to create a nonadhesive culture surface for optimal tissue remodeling (29). The Pluronic F-127 solution was aspirated before cell seeding.

## Polymethyl Methacrylate Culture Device Fabrication

The polymethyl methacrylate (PMMA) hMMT culture device was fabricated as described (23), and generously provided by ArtifiCell GmbH. In brief, the device comprises a chamber and a lid, both milled from PMMA. The chamber contained eight ellipsoid-shaped culture wells and was affixed to a standard microscopy coverslip using PDMS. The PMMA lid, designed with 16 elongated, ellipsoid-shaped posts—two extending into opposite sides of each well—was placed atop the chamber. Eight holes, positioned between each pair of posts, facilitated media and gas exchange. Additional holes, each located behind a post, allowed for the insertion of electrodes for EFS. Before use, the device was sterilized with 70% ethanol and subsequently coated with a 5% Pluronic F-127 solution diluted in dH<sub>2</sub>O, which was aspirated before cell seeding.

## Human Primary Myoblast Preparation and Culture

Primary myoblast cell lines derived from the skeletal muscle of three healthy human donors were used for the fabrication of hMMTs in the MyoTACTIC culture platform. The muscle group from which the biopsies were obtained and the sex, age, and weight or body mass index (BMI) of the biopsy donors are given in Table 1. Cell line 1 (CL1; SK-1111-P01358-19F) and cell line 3 (CL3; SK-1111-P01236-18M) were purchased from Cook MyoSite Inc. (Pittsburgh, PA), where cell lines were prepared using a proprietary method.

Cell line 2 (CL2) was derived from human gracilis skeletal muscle tissue collected within 4 h of death from a cadaveric donor with no history of arthritis, joint injury, or surgery, no prescription of anti-inflammatory medications, and no comorbidities. Consent was obtained from next of kin. The collection and use of human skeletal muscle tissue was reviewed and approved by the University of Calgary Research Ethics Board (REB15-0005). The University of Toronto Office of Research Ethics also reviewed and approved this study and assigned administrative approval (Protocol No. 34888). All procedures in this study were performed in accordance with the guidelines and regulations of both Research Ethics Boards. CL2 was established and maintained in culture as described (30). Briefly, following receipt of biopsy tissue by the University of Toronto research laboratory, the muscle was minced, enzymatically digested with collagenase clostridium histolyticum (630 U/mL; Cat. No. C9891, Sigma) and dispase (0.03 U/mL; Cat. No. 17105041, Gibco; Waltham, MA), and passed through a 20-G needle to release myogenic progenitor and other tissue resident mononucleated cell populations. Red blood cells were lysed by incubation with lysis buffer, containing 15.5 mM NH<sub>4</sub>Cl, 1 mM KHCO<sub>3</sub>, and 10  $\mu$ M EDTA. The remaining cells,

primarily consisting of myogenic progenitors and fibroblast-like cells, were then transferred to a collagen-coated tissue culture dish (Cat. No. 25382-442, Corning; Corning, NY) for attachment and expansion. Cells were cultured in primary myoblast growth medium consisting of Ham's F-10 nutrient mix (Cat. No. 318-050-CL, Wisent Bioproducts; Saint-Jean Baptiste, Quebec, Canada) supplemented with 20% fetal bovine serum (FBS; Cat. No. 12483020, Gibco), 5 ng/mL basic fibroblast growth factor (bFGF; Cat. No. 11343625, ImmunoTools; Friesoythe, Germany), and 1% Penicillin-Streptomycin (P/S; Cat. No. 15140122, Gibco). The medium was refreshed every 2–3 days. After one passage, the cells were immunostained with an antibody recognizing neural cell adhesion molecule (CD56; Cat. No. 557711, BD Pharmingen; Franklin Lakes, NJ). The CD56<sup>+</sup> myogenic progenitors were then purified using fluorescence-activated cell sorting. The CD56<sup>+</sup> cell population was maintained on collagen-coated tissue culture dishes in the growth medium until passage 8 and was then used for hMMT seeding in MyoTACTIC.

## Human Immortalized Myoblast Culture

The AB1167 human immortalized myoblast cell line, derived using the MyoLine cell culture platform at the Institut de Myologie (Paris, France), was used for the fabrication of hMMTs in the MyoTACTIC and PMMA culture chamber platforms. Immortalized myoblasts were expanded as previously described (14, 28). In brief, the cells were maintained on tissue culture dishes in immortalized myoblast growth medium consisting of the Skeletal Muscle Cell Growth Medium kit (Skeletal Muscle Cell Basal Medium with Skeletal Muscle Cell Growth Medium Supplement Mix; Cat. No. 23060, PromoCell; Heidelberg, Germany) with 15% FBS and 1% P/S. The medium was refreshed every 2 days. The cells were passaged until the population was sufficiently expanded for hMMT seeding in the MyoTACTIC model or PMMA culture chambers.

## Myogenic Differentiation of Human Induced Pluripotent Stem Cells

Generation of the previously reported induced pluripotent stem cell (iPSC) line LiPSC-GR1.1 (also referred to as TC1133 or RUCDRi002-A; Lot Number 50-001-21) was supported by the National Institutes of Health (NIH) Common Fund Regenerative Medicine Program (31). The NIH Common Fund and the National Center for Advancing Translational Sciences are joint stewards of the LiPSC-GR1.1 resource. Repairon GmbH acquired and imported a vial from the TC1133 master cell bank, from which a Working Cell Bank (WCB) was created. Myriamed GmbH acquired a derivative of the WCB from Repairon GmbH and provided a non-GMP derivative thereof to the Institute of Pharmacology and Toxicology at the University Medical Center Göttingen for noncommercial research use.

Differentiation of TC1133 iPSCs into myogenic progenitors was performed on matrigel-coated flasks (1:120 dilution in phosphate buffered saline; Cat. No. 354230, Corning) as recently reported (32, 33). Briefly, iPSCs were expanded for 24 h in StemMACS iPS-Brew XF medium (Cat. No. 130-104-368, Miltenyi Biotec; Bergisch Gladbach, Germany) containing 5  $\mu$ mol/L of Y27632 (Cat. No. 040012-10, Stemgent;

**Table 1.** Characteristics of the skeletal muscle biopsy donors and the muscle group from which the biopsies were derived for the three primary cell lines

	Cell Line 1	Cell Line 2	Cell Line 3
Sex	Female	Male	Male
Age, yr	19	64	18
Body weight or BMI*	24*	85 kg	21*
Muscle	Vastus lateralis	Gracilis	Rectus abdominus

\*Body mass index (BMI) = kg/m<sup>2</sup>.



Cambridge, MA) to reach 30% culture confluency. Paraxial mesoderm induction, myogenic specification, and myogenic expansion were then performed over 3 wk. All media were formulated based on N-2 basal medium consisting of low glucose (1 g/L) Dulbecco's modified Eagle's medium (DMEM; Cat. No. 10567014, Gibco) supplemented with 1% N-2 Supplement (Cat. No. 17502048, Gibco), 1% minimum essential media (MEM) nonessential amino acid solution (Cat. No. 11140035, Gibco), and 1% P/S. Media was refreshed daily.

From *day 0* to *day 3*, iPSCs were maintained in N2-CLF medium, composed of N-2 basal medium with 10  $\mu\text{mol/L}$  CHIR99021 (Cat. No. 04-0004, Stemgent), 0.5  $\mu\text{mol/L}$  LDN193189 (Cat. No. 04-0074, Stemgent), and 10 ng/mL FGF-2 (Cat. No. AF-100-18B, PeproTech; Cranbury, NJ). On *days 4* and *5*, the medium was replaced with N-2 basal medium, 20 ng/mL FGF-2, and 10  $\mu\text{mol/L}$  gamma secretase inhibitor (DAPT; Cat. No. 2634, Tocris; Bristol, UK), referred to as N2-FD medium. On *days 6* and *7*, iPSCs were cultured in N2-FDH medium, consisting of N2-FD supplemented with 10 ng/mL hepatocyte growth factor (HGF, Cat. No. 100-39, Peprotech). From *day 8* to *day 11*, the medium was exchanged to N-2 basal medium with 10  $\mu\text{mol/L}$  DAPT, 10 ng/mL HGF, and 10% knockout serum replacement (Cat. No. 10828028, Gibco), referred to as N2-DHK medium. Finally, from *day 12* to *day 21*, the cells were expanded in N2-HK composed of N-2 basal medium, containing 10 ng/mL HGF and 10% knockout serum replacement. The myoblasts were then enzymatically dissociated with TrypLE (Cat. No. 12604021, Gibco) for 5–8 min at 37°C and used for hMMT seeding in PMMA culture chambers.

### hMMT Production in MyoTACTIC

Three-dimensional hMMTs in MyoTACTIC were generated as described (14, 17, 28). Briefly, myoblasts were resuspended in a hydrogel mixture of 4 mg/mL fibrinogen (40% vol/vol; Cat. No. F8630, Sigma) and Geltrex (20% vol/vol; Cat. No. A1413202, Gibco) in high glucose (4.5 g/L) DMEM (40% vol/vol; Cat. No. 11995065, Gibco). Human primary and immortalized myoblasts were resuspended at  $1.5 \times 10^7$  and  $1.0 \times 10^7$  cells/mL of hydrogel mixture, respectively. Thrombin (Cat. No. T6884, Sigma) was added to the cell-hydrogel suspension at 0.37 U/mg of fibrinogen. Subsequently, 15  $\mu\text{L}$  of this mixture (containing  $2.25 \times 10^5$  cells/tissue for primary hMMTs and  $1.50 \times 10^5$  cells/tissue for immortalized hMMTs) was carefully pipetted into each well of an autoclaved, Pluronic acid-coated MyoTACTIC culture plate to engineer one hMMT per well. The mixture was carefully distributed between and around the vertical microposts at either end of the culture well to avoid formation of air bubbles, then the seeded wells were incubated for 5 min at 37°C to promote thrombin-mediated fibrinogen cleavage into fibrin.

Once the fibrin had polymerized, the MyoTACTIC culture wells were filled with 200  $\mu\text{L}$  of “after seeding” growth medium. For primary hMMTs, after seeding growth medium was composed of Ham's F-10 nutrient mix supplemented with 20% FBS, 1.5 mg/mL 6-aminocaproic acid (ACA; 3% vol/vol; Cat. No. A2504, Sigma), and 1% P/S. For immortalized hMMTs, Skeletal Muscle Cell Basal Medium replaced Ham's F-10 nutrient mix in the after seeding medium. Two days later, the culture media was exchanged for differentiation

medium, containing high-glucose DMEM supplemented with 2% horse serum (HS; Cat. No. 16050114, Gibco), 2 mg/mL ACA (4% vol/vol), 10  $\mu\text{g/mL}$  insulin (Cat. No. 91077 C, Sigma), and 1% P/S. Primary and immortalized hMMTs were maintained in differentiation medium for 14 days and 12 days, respectively. Half of the media was replaced every other day. A summary of all media used in the expansion of human primary and immortalized myoblast lines, and differentiation of iPSCs into myogenic progenitors can be found in Supplemental Table S1.

### hMMT Production in PMMA Culture Device

Three-dimensional hMMTs in PMMA culture devices were generated as described (23). Briefly, human immortalized and iPSC-derived myoblasts were resuspended in the hydrogel mixture outlined above at  $1.2 \times 10^7$  and  $6 \times 10^6$  cells/mL, respectively. Thrombin was added to the cell-hydrogel suspension at 0.50 U/mg of fibrinogen. Subsequently, 25  $\mu\text{L}$  of this mixture (containing  $3.00 \times 10^5$  cells/tissue for immortalized hMMTs and  $1.50 \times 10^5$  cells/tissue for iPSC-derived hMMTs) was carefully pipetted into each well of a sterilized, Pluronic acid-coated PMMA culture chamber to engineer one hMMT per well. The lid was placed atop the chamber, then the seeded wells were incubated for 5 min at 37°C.

Once the fibrin had polymerized, immortalized hMMTs were cultured in 300  $\mu\text{L}$  “after seeding” growth medium composed of Skeletal Muscle Cell Growth Medium supplemented with 15% FBS, 1.5 mg/mL ACA, and 1% P/S. Two days later, the culture media was exchanged for differentiation medium, containing low-glucose DMEM supplemented with 2% HS, 2 mg/mL ACA, 10  $\mu\text{g/mL}$  insulin (Cat. No. 91077 C, Sigma), and 1% P/S. Immortalized hMMTs were maintained in differentiation medium for 12 days before use. The media was refreshed every other day.

Once the fibrin had polymerized, iPSC-derived hMMTs were cultured in 300  $\mu\text{L}$  of N-HK expansion medium supplemented with 5  $\mu\text{mol/L}$  Y27632 and 1.5 mg/mL ACA. The following day, the medium was replaced with N-HK expansion medium containing 1.5 mg/mL ACA alone, and refreshed every other day. After 1 week, the medium was exchanged for fusion maturation medium, consisting of low glucose (1 g/L) DMEM, 1% N-2 Supplement, 2% B-27 Supplement (Cat. No. 17504044, Gibco), and 1% P/S, supplemented with 0.1  $\mu\text{mol/L}$  Triiodo-L-thyronine (T3; Cat. No. T2877, Sigma), 1  $\mu\text{mol/L}$  SCH772984 (Cat. No. 19166, Cayman Chemical; Ann Arbor, MI), and 2 mg/mL ACA. iPSC-derived hMMTs were maintained in fusion maturation medium for 3 weeks before use. The media was refreshed every other day. A summary of all media and solutions used in the preparation and culture of hMMTs seeded in MyoTACTIC and PMMA culture chamber platforms can be found in Supplemental Table S2.

### hMMT Electrical Field Stimulation in MyoTACTIC

Electrical field stimulation of hMMTs was performed on *day 12* and *day 14* of differentiation for immortalized and primary hMMTs, respectively, as described (14, 17, 28). Briefly, electrodes fabricated from sterile syringe needles (25-G  $\times$  5/8 in.; Cat. No. 305122, BDTM; Franklin Lakes, NJ) were inserted into the well, one behind each micropost. Needles were wrapped with tin-coated copper wires (Cat. No. 30TCW,

Remington Industries; Johnsburg, IL) and connected to a pulse generator (DG1022U, Rigol; Suzhou, PR China) with alligator clamps. Square-wave pulses were thereby generated in an electrical field oriented parallel to the hMMT. Videos of micropost deflection were captured with an iPhone SE (Apple; Cupertino, CA) secured by an iPhone microscope mount (LabCamR; Detroit, MI) on the eyepiece of an Olympus IX83 inverted microscope (Tokyo, Japan) using the  $\times 10$  objective. For each hMMT, deflection of the two microposts during EFS was initially confirmed by visual inspection, and the micropost with the greatest deflection was recorded at 30 frames/s during the experiment.

### hMMT Electrical Field Stimulation in PMMA Culture Device

Electrical field stimulation of hMMTs was performed on *day 12* of differentiation for immortalized hMMTs and *day 28* of maturation for iPSC-derived hMMTs. Electrodes fabricated from metal pins (0.55 mm diameter; Cat. No. 26001-55, Fine Science Tools; Foster City, CA) were inserted through the holes behind each micropost in the PMMA lid. Pins were wrapped with copper wires that were directly connected to a multifunction input/output unit (Model USB-6001; Cat. No. 782604-01, National Instruments; Austin, TX). The unit was operated via a custom Python graphical user interface program (34). Videos of micropost deflection were recorded with a Nikon Eclipse Ti-E inverted microscope (Tokyo, Japan) equipped with a scientific complementary metal-oxide-semiconductor camera (Prime BSI, Photometrics; Tucson, AZ) using the  $\times 20$  objective. For each hMMT, deflection of the two microposts during EFS was initially confirmed by visual inspection, and the micropost with the greatest deflection was recorded during the experiment.

### Analysis of hMMT Contractions

Videos capturing micropost movement, produced by contractions of hMMTs cultured in MyoTACTIC, were analyzed as described (17, 28). Briefly, the videos were processed by a custom Python script, available on GitHub (35), which detects the position of the micropost in each frame and computes the displacement for contractions from these raw post positions. Displacement values in pixels were then converted to movement in microns and contractile force in Newtons using a pixel-to-distance and distance-to-force conversion factor, respectively (17).

Videos capturing micropost movement, produced by contractions of hMMTs cultured in the PMMA device, were analyzed with a script using a novel edge detection algorithm. In this algorithm, the edge of the micropost is detected in each frame using a multiscale approach. Specifically, the magnitude of the image gradient is calculated across different resolutions by applying derivative-of-Gaussian kernels with several widths. Edge locations are expected to produce high gradient magnitude values across multiple scales. Thus, the image gradients are aggregated across different resolutions to enhance detection accuracy in the algorithm. The edge positions are retrieved by sliding a perpendicular line profile along the direction of the edge, across the aggregated gradient magnitudes, and collecting the positions of the peak intensity values. Subpixel edge localization is achieved by fitting a quadratic function to the collected positions using robust

regression. The micropost displacement values for contractions were then extracted from the time course of fitted edge positions using the same Python script used in hMMTs cultured in MyoTACTIC (17), and which is available on GitHub (35). Finally, the displacement values in pixels were converted to contractile forces in Newtons by multiplication with the apparent spring constant of the microposts, as done previously (23).

For a tetanic contraction, the maximum force achieved during contraction is reported. For trains of stimuli, we report twitch, dynamic oscillation of force (DOF), and absolute force values, where absolute force is the difference between the initial resting baseline and the peak displacement induced by a given stimulus. Twitch force is defined as the maximum force above resting force induced by the first stimulus in the train of stimuli delivered at 0.5 Hz or 1 Hz. DOF values represent the difference between the peak and nadir force during stable rhythmic contractions and were determined by averaging data obtained from the third, fourth, and fifth contractions in the train. In some video recordings, the microposts could not be accurately identified and/or tracked by the Python script (e.g., if micropost edges appeared blurry). These cases were analyzed for a train of stimuli or single tetanic stimulus by capturing screenshots of the micropost in the relaxed and contracted state, importing them into ImageJ software (NIH; Bethesda, MD), and using the line tool followed by the measure function to quantify micropost movement.

To evaluate the kinetics of hMMT contraction, we measured time-to-peak tension (TPT), half-relaxation time (1/2 RT), contraction rate (CR), relaxation rate (RR), full-width at half-maximum force (WHM), and duration-at-peak (DP) for twitch and DOF. Respective metrics, apart from duration-at-peak, are used to evaluate the kinetics of native skeletal muscle contraction (36–38). For twitch kinetics, values for the first contraction elicited in response to the train of stimuli delivered at 0.5 Hz or 1 Hz were reported. For DOF, the average kinetics value for the third, fourth, and fifth contractions was reported. These metrics were calculated using a custom Python script available on GitHub (35). The script operates by identifying key stages of contraction from the time course of micropost/fitted edge positions for contractions elicited by hMMTs. The key stages of contraction are the start of contraction (P1), mid-contraction (P2), beginning of peak (P3), end of peak (P4), mid-relaxation (P5), and termination of contraction (P6). The illustration associated with Supplemental Table S4 depicts these six positions along with the associated kinetics metric.

The script uses a defined algorithm to determine the frame numbers corresponding to the six contraction stages from the time course of micropost/fitted edge positions. To identify P2 and P5, the algorithm calculates the deflection of the micropost halfway from P1 to the peak, and from the peak to P6, respectively. The script selects the frame at which the micropost reaches the calculated deflection. If a frame does not capture the exact deflection value, the next frame following the half-way point is chosen. For contractions without a plateau at the peak, the script assigns the same frame number to both P3 and P4.

## Optimization of Voltage and Pulse Duration for hMMT Contractions

For primary and iPSC-derived hMMTs cultured in the MyoTACTIC and PMMA platforms, respectively, the stimuli train conditions eliciting peak twitch force and DOF during 1 Hz stimulations were identified. For immortalized hMMTs cultured in both the MyoTACTIC and PMMA platforms, the stimuli train conditions eliciting peak twitch force during 0.5 Hz stimulations were identified. For each line, three hMMTs were stimulated at 0.5 Hz or 1 Hz with pulse durations ranging from 1 ms up to 100 ms as specified in the text; voltage was increased from 1 V up to 10 V by 1 V increments. Microtissues were stimulated to contract 6 or 7 times at each combination of parameters for a total of 60–70 contractions per microtissue through the range of voltages.

EFS of hMMTs cultured in the MyoTACTIC platform was performed at room temperature (RT, 23°C–25°C). For primary hMMTs, MyoTACTIC portions containing the hMMTs were removed from the 37°C incubator and equilibrated for 10 min in an environmental chamber (INUBTFP controller, GM-8000 digital gas mixer, and IX3WX stage top incubator; Tokai Hit; Fujinomiya, Japan) at 25°C and 5% CO<sub>2</sub>. The MyoTACTIC portion was then removed from the chamber and placed on a glass slide secured on the microscope stage in preparation for EFS. For immortalized hMMTs, the MyoTACTIC portion was transferred directly from the incubator to the microscope stage without prior equilibration. Electrodes were then positioned (~3 min), and all the hMMTs in the MyoTACTIC portion were consecutively stimulated at RT. Each of three hMMTs was stimulated at a designated pulse duration through the range of voltages before the next pulse duration was assessed. For primary CL2 and CL3, and immortalized hMMTs, MyoTACTIC portions contained 3–6 hMMTs and required ≥30 min for the stimulation protocol, whereas CL1 MyoTACTIC portions contained three hMMTs necessitating <30 min.

EFS of immortalized and iPSC-derived hMMTs cultured in the PMMA device was conducted on a microscope stage housed within a temperature-controlled cage incubator (enclosure chamber and temperature unit; Okolab; Pozzuoli, Italy) set to 37°C. The device was first removed from the incubator and secured on the microscope stage. Electrodes were then positioned (~3 min), and one hMMT in the PMMA device was stimulated at a designated pulse duration through the range of voltages. After EFS, the device was returned to the incubator for ~20 min to allow for video file processing before the next hMMT in the PMMA device was stimulated.

## Effect of Stimulation Frequency on DOF and Absolute Force

To study the effect of stimulation frequency on DOF and absolute force, hMMTs generated from the three primary myoblast cell lines in the MyoTACTIC platform were used. In these experiments, DOF and absolute force were measured for primary hMMTs stimulated at 60 ms and 5 V as stimulation frequency was increased from 0.25 to 2 Hz by 0.25 Hz increments. Microtissues were induced to contract 6 or 7 times at each combination of stimulation parameters for a total of 48–56 contractions per microtissue through the range of frequencies. Primary hMMTs were stimulated at RT immediately

after removal from the cell culture incubator and required ~10 min for analysis. For each cell line, three technical replicates were assessed. For CL2 and CL3, individual hMMTs within a single MyoTACTIC portion served as technical replicates. The MyoTACTIC portion was placed in the cell culture incubator for a 10-min period after each hMMT was analyzed to allow for rewarming at 37°C and then studied at RT. For CL1, hMMTs from different MyoTACTIC portions served as technical replicates, which eliminated the rewarming step, as each hMMT was studied separately at RT.

## Evaluation of hMMT Frequency-Force Relationship and Force Production

For primary hMMTs cultured in the MyoTACTIC platform, and immortalized and iPSC-derived hMMTs cultured in the PMMA device, the stimulation frequency eliciting peak tetanic force was identified. Absolute force was measured for hMMTs stimulated at the optimal voltage (i.e., peak twitch force voltage) as frequency was increased from 0.5 or 1 Hz up to 50 or 100 Hz. EFS was performed at 1 Hz increments from 1 to 10 Hz, 5 Hz increments from 10 to 50 Hz, and 10 Hz increments thereafter. At 0.5 Hz or 1 Hz, EFS was applied with the optimal pulse duration (i.e., that used for peak twitch force). Pulse duration was reduced to 10 ms at higher frequencies to minimize tissue fatigue (39). Visual inspection of a separate tissue was used to identify a suitable pulse duration at stimulation frequencies >0.5 Hz or 1 Hz; the shortest pulse duration eliciting the greatest micropost deflection at a given frequency was selected. At each frequency, hMMTs were stimulated for 5 s with 20-s rest in between. For each cell line, 3–5 technical replicates were assessed. hMMTs were stimulated at RT (MyoTACTIC) or in a 37°C temperature-controlled cage incubator (PMMA device) immediately after removal from the incubator as described earlier in *Effect of Stimulation Frequency on DOF and Absolute Force*.

## Statistical Analysis

The number of technical replicate hMMTs ( $n$ ) and biological replicate experiments ( $N$ ) is indicated in the figure legends. Values are reported as the means ± standard deviation (SD). Error bars and a gray shaded region are used to represent SD in bar graphs and line graphs, respectively. One-way ANOVA followed by Tukey's tests were used to assess statistically significant differences between groups with  $P \leq 0.05$ . Details of technical replicates, statistical tests, and  $P$  values for each set of experiments are given in Supplemental Table S3. GraphPad Prism 8.0 (GraphPad Software; Boston, MA) was used to create all graphs and perform statistical analysis.

## RESULTS

### Peak Twitch Force of Primary hMMTs Is Elicited at 5 V, 60-ms Pulse Duration

We first evaluated the stimulus conditions to determine the length of time from the beginning to the end of each stimulus (i.e., pulse duration, ms) and electrical field strength (i.e., volts, V), that induce primary hMMT peak twitch force during stimulation at 1 Hz. hMMTs cultured in MyoTACTIC were stimulated through a range of 1–10 V at pulse durations



ranging from 1 ms to 80 ms (Fig. 1A). Across all three cell lines, higher voltages and longer pulse durations produced greater force (Fig. 1, B, D, and F). Voltages below 2 V were not sufficient for hMMTs to generate micropost movement at any pulse duration and higher voltages were required to generate trackable micropost movement at shorter pulse durations. Electrolysis during EFS > 5 V caused the media to become murky with bubbles gradually obscuring optical tracking over successive contractions. Force measurements at 6–7 V could be tracked, but once voltage was increased to 8 V, the post was obscured. Electrolysis did not occur with repeated stimulations at 5 V, which thereby defined it as our standard. When varying pulse duration, CL1 (Fig. 1B) and CL2 hMMTs (Fig. 1D) produced peak twitch force at 60 ms. Although CL3 hMMTs developed peak twitch force at 80 ms, trend lines for CL3 at 60 ms and 80 ms intersect at 7 V (Fig. 1F). These data lead to 60 ms as the optimal pulse duration for hMMTs. The three technical replicates of each cell line varied in twitch force

(Fig. 1, C, E, and G). A time control showed that peak twitch force decreases by 76% over a 30-min period at RT following the initial 10-min equilibration (Supplemental Fig. S1). Given that replicates in each MyoTACTIC portion were stimulated consecutively without rewarming, a loss of force over time may have contributed to variability between replicates. Nevertheless, averaging across replicates identified consistent trends between hMMTs from the different lines of myoblasts used to generate hMMTs (Fig. 1, B, D, and F).

From these experiments, we conclude that hMMTs from the three myoblast lines should be stimulated at 5 V and 60 ms for the evaluation of peak twitch force in the MyoTACTIC platform. Under these stimulation conditions, CL1, CL2, and CL3 hMMTs produced a mean peak twitch force of  $41.1 \pm 11.4 \mu\text{N}$ ,  $40.1 \pm 20.0 \mu\text{N}$ , and  $79.2 \pm 11.4 \mu\text{N}$ , respectively ( $n = 3$  hMMTs per cell line; Supplemental Fig. S2). The differences in force between CL1 and CL3 hMMTs, and CL2 and CL3 hMMTs, were statistically significant ( $P = 0.046$  and  $P = 0.041$ , respectively;

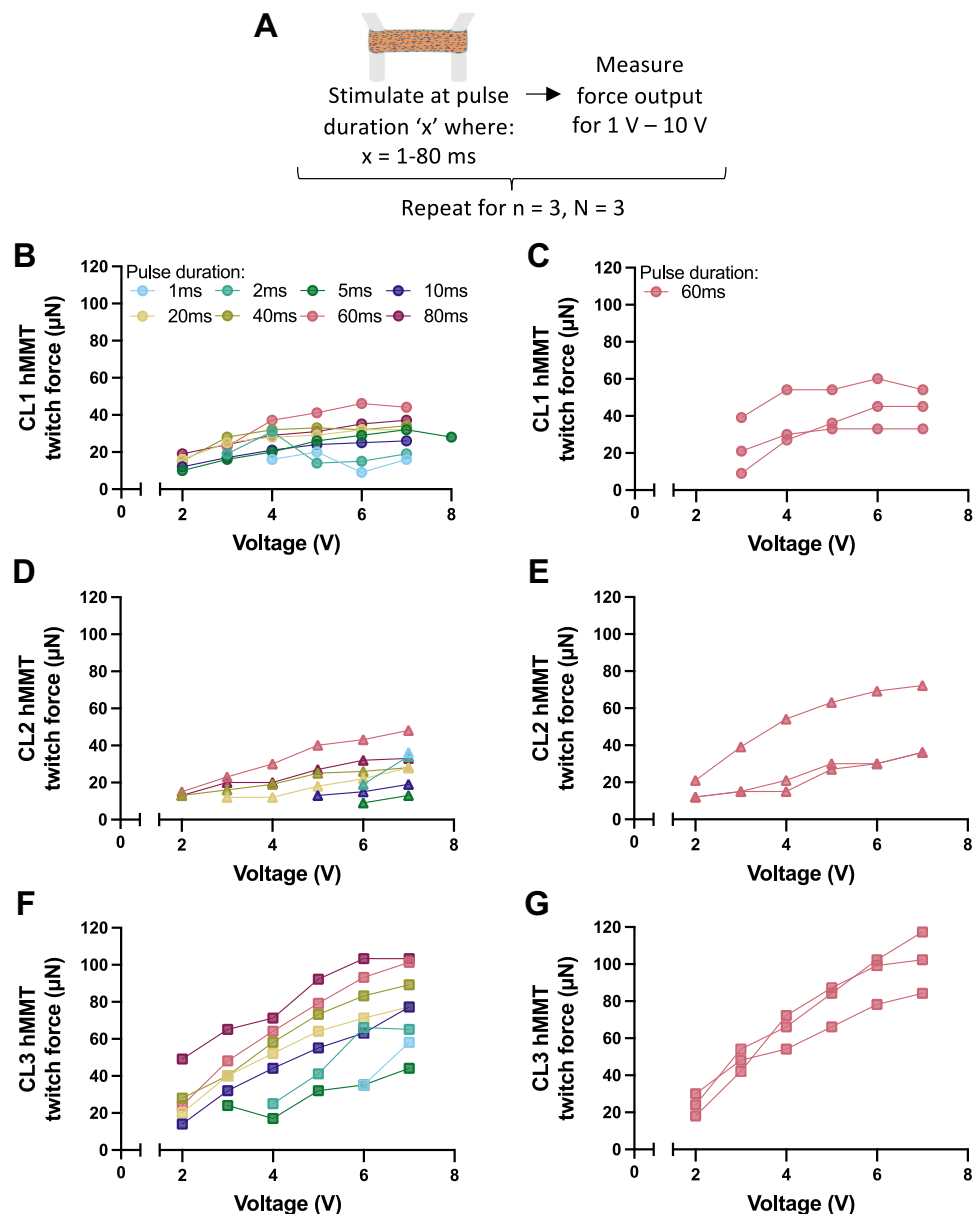


**Figure 1.** Optimization of voltage and pulse duration for peak twitch force. **A:** experimental design. Primary human skeletal muscle microtissues (hMMTs) cultured in MyoTACTIC were stimulated at 1 Hz and pulse durations ranging from 1 ms to 80 ms as voltage was increased from 2 V up to 8 V by 1 V increments. Data in (B), (D), and (F) show mean values for  $n = 3$  hMMTs. Force produced by individual hMMT technical replicates are shown for cell line 1 (CL1, C), for cell line 2 (CL2, E), and for cell line 3 (CL3, G) stimulated at 1 Hz and 60 ms.

one-way ANOVA). These experiments underscore the importance of optimizing the stimulation parameters for evaluating force production in human primary myoblast-derived microtissues to make comparisons between biological replicates.

### Dynamic Oscillation of Force of Primary hMMTs Is Reduced as Absolute Force Is Increased

During repetitive stimulation at 1 Hz, the first contraction elicited by primary hMMTs cultured in MyoTACTIC was consistently the weakest; peak force increased during the second and third contractions, stabilizing by the fourth contraction. The force tracks produced in response to the trains of stimuli indicate that this increase in force during the initial contractions is attributable to summation. The failure of force to return to baseline between each stimulus during the train precludes accurate determination of twitch force from these subsequent contractions. We thereby introduce a metric, termed the dynamic oscillation of force (DOF), which defines the difference between minimal and peak force values in a train of stimuli following stabilization of contraction oscillations (Fig. 2A). We suggest that DOF provides a dynamic index of hMMT contraction and relaxation that complements the kinetics of contraction and relaxation of a single twitch.

We anticipated that there should be more summation and lower DOF values with less time for relaxation between successive stimuli as frequency increases until fused tetanus is

reached (i.e., when DOF equals zero). Consistently, representative hMMT force records at 1 Hz (Fig. 2B) and 2 Hz (Fig. 2C) showed an inverse relationship between DOF and stimulation frequency. This relationship is further supported by summary data averaged across cell lines for DOF (Fig. 2D) and absolute force (Fig. 2E). The decreases in DOF and increases in absolute force were most prominent above 1 Hz, as is evident from the slope of the trend lines. Because micropost oscillation produced by hMMT stimulation >2 Hz was too rapid to be reliably captured by video recording at 30 frames/s, the assessment of DOF was limited accordingly.

### Peak Dynamic Oscillation of Force of Primary hMMTs Is Elicited at 1 Hz, 5 V, 60-ms Pulse Duration

DOF values were measured from the force tracks elicited at each combination of stimulus parameters tested for systemic optimization. Similar trends were observed for twitch force, but notable distinctions justify the use of DOF in the analysis of hMMTs (Fig. 3, Supplemental Fig. S3). First, DOF quantifies the oscillation between the peak and nadir of force production at defined stimulus conditions. At the optimized stimulation parameters for primary hMMTs (1 Hz, 5 V, 60 ms), CL1, CL2, and CL3 produced peak DOF forces of  $55.5 \pm 14.7 \mu\text{N}$ ,  $55.2 \pm 25.2 \mu\text{N}$ , and  $121.0 \pm 29.4 \mu\text{N}$ , respectively ( $n = 3$  hMMTs per cell line; Supplemental Fig. S4). Second, DOF plateaued at the highest voltage compatible with EFS in

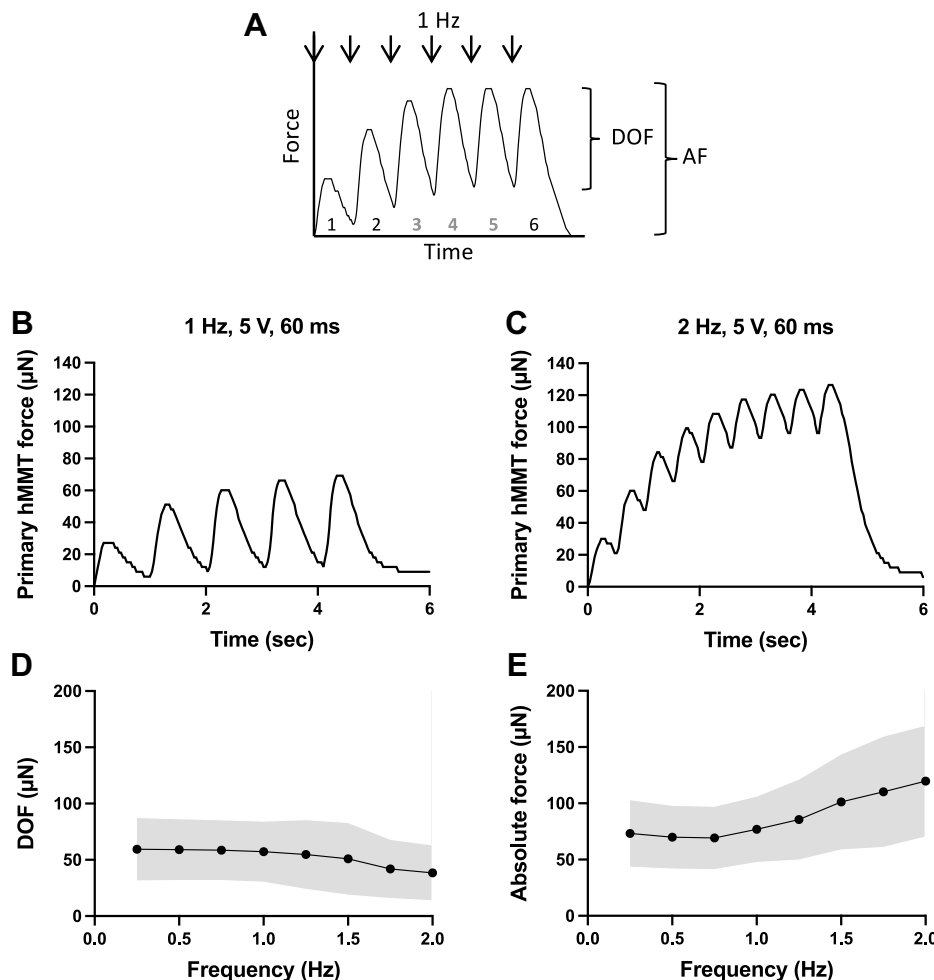


**Figure 2.** Dynamic oscillation of force (DOF) and absolute force (AF) for stimulation frequencies up to 2 Hz. A: graphical representation of the DOF and AF analysis parameters derived from a representative twitch force track elicited by primary human skeletal muscle microtissues (hMMTs) cultured in MyoTACTIC. Arrows indicate successive stimuli at 1 Hz stimulation. Representative force tracks for contractions produced at 1 Hz (B) and 2 Hz (C) stimulation frequencies with 60-ms pulse duration by primary hMMTs. At 2 Hz, summation produces an unfused tetanus and reduces DOF. DOF (D) and absolute force (E) averaged for cell line 1, cell line 2, and cell line 3 hMMTs elicited at 60 ms and 5 V as frequency was increased from 0.25 Hz to 2 Hz in 0.25 Hz increments. D and E: data show means  $\pm$  SD (shaded regions) for  $n = 9$  hMMTs (with  $n = 3$  hMMTs from each of the three cell lines).



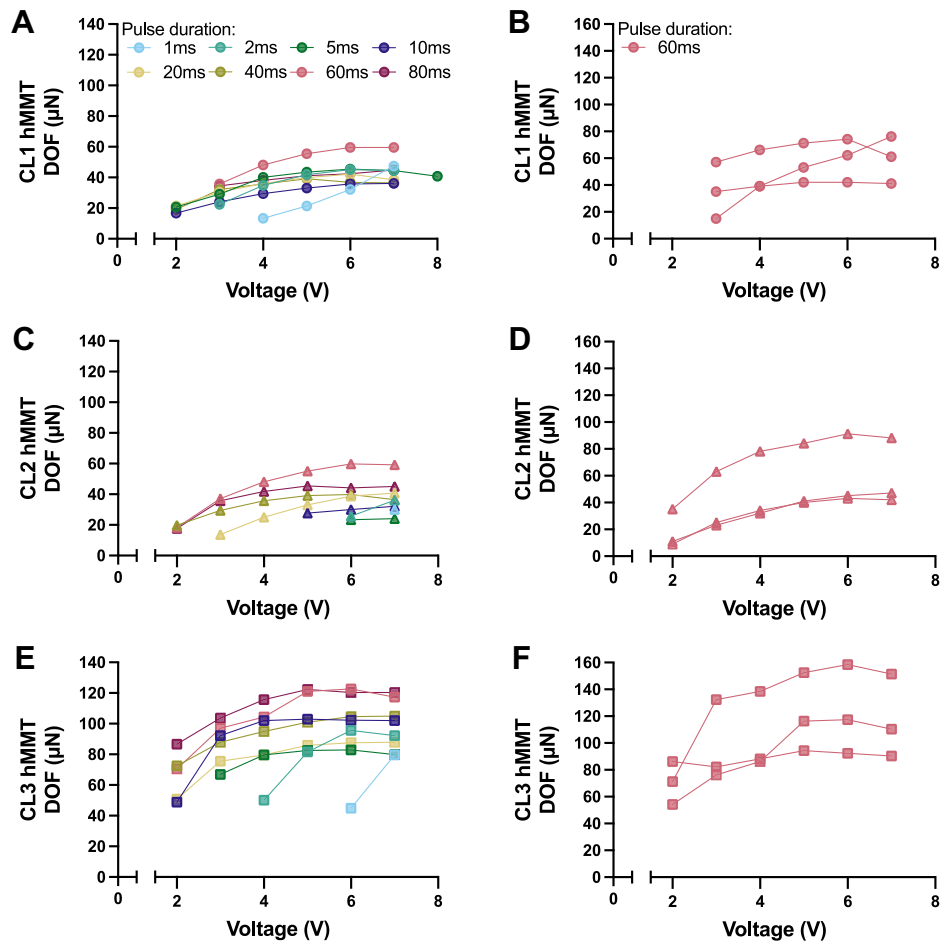


**Figure 3.** Optimization of voltage and pulse duration for peak dynamic oscillation of force (DOF) at 1 Hz. The DOF produced by primary human skeletal muscle microtissues (hMMTs) cultured in MyoTACTIC at 1 Hz and pulse durations ranging from 1 ms to 80 ms as voltage was increased from 2 V to 8 V in 1 V increments. The hMMTs were generated from cell line 1 (CL1) in (A), from cell line 2 (CL2) in (C), and from cell line 3 (CL3) in (E). Data are mean values for  $n = 3$  hMMTs in each panel. DOF produced by individual hMMT technical replicates are shown for CL1 (B), for CL2 (D), and for CL3 (F). hMMTs were stimulated 1 Hz and 60 ms.

the MyoTACTIC platform. Notably, EFS of CL3 hMMTs with pulse durations of 60 ms and 80 ms produced similar DOF values from 5 to 7 V. The DOF data thereby support 5 V, 60 ms as optimal stimulation parameters for the hMMTs tested here. In practice, DOF evaluates a dynamic of the contraction-relaxation cycle in response to a train of stimuli that complements values obtained for a single-twitch contraction.

### DOF Contraction Kinetics Trend Faster than Twitch Contraction Kinetics

We next evaluated the kinetics of twitch and DOF contractions elicited by EFS at 1 Hz, 60 ms through the range of 3–7 V. Trends for time-to-peak tension, half-relaxation time, contraction rate, relaxation rate, and full-width at half-maximum for DOF are consistent with those for twitch contractions (Fig. 4, A–F). For twitches, time-to-peak contraction and half-relaxation times are similar (Fig. 4A). For DOF, time-to-peak contraction tends to be faster than half-relaxation time (Fig. 4B). The contraction and relaxation rates for DOF trend faster than those for twitch, with contraction rates consistently exceeding relaxation rates (Fig. 4, C and D). Contraction and relaxation rates increased through 6 V then plateaued or slightly decreased at 7 V (Fig. 4, C and D). Accordingly, the full width at half-maximum for twitch slightly decreased up to 7 V (0.503–0.486 s), whereas that for DOF slightly decreased up to 6 V (0.561–0.508 s), and

increased thereafter (Fig. 4, E and F). Finding that hMMTs appear to maintain peak force before relaxation, we introduce a new kinetics metric, the duration-at-peak, which tended to decrease between 3 and 5 V (Fig. 4, G and H).

The kinetics for twitch and DOF contractions revealed similar patterns across all assessed metrics and uncovered the tendency of DOF contraction kinetics to trend faster, which aligns with DOF reporting the maximum oscillation of force for a set of stimulus conditions. Notably, although our system does not support repeated EFS above 5 V, the present data suggest that application of a stronger electric field may not be optimal for the evaluation of hMMT contractile function. The DOF kinetics of CL1, CL2, and CL3 hMMTs at the EFS parameters eliciting peak DOF are provided in Supplemental Table S4.

### Peak Tetanic Force of Primary hMMTs Is Elicited at 7 Hz, 5 V, 10-ms Pulse Duration

We evaluated the relationship between stimulus frequency and force production to define the frequency that elicits peak tetanic force from primary hMMTs. Force tracks were measured from baseline to peak at stimulation frequencies ranging from 1 Hz to 50 Hz (Fig. 5A). The frequency-force relationship was evaluated at 5 V, as this is the highest voltage compatible with repeated EFS in the MyoTACTIC platform. Peak tetanic force was elicited at 7 Hz, 10 ms for hMMTs from each cell line (Fig. 5B). CL1, CL2, and CL3 hMMTs produced an average peak force of  $111.7 \pm 30.4 \mu\text{N}$  ( $n = 5$  hMMTs),  $177.7 \pm 49.5 \mu\text{N}$

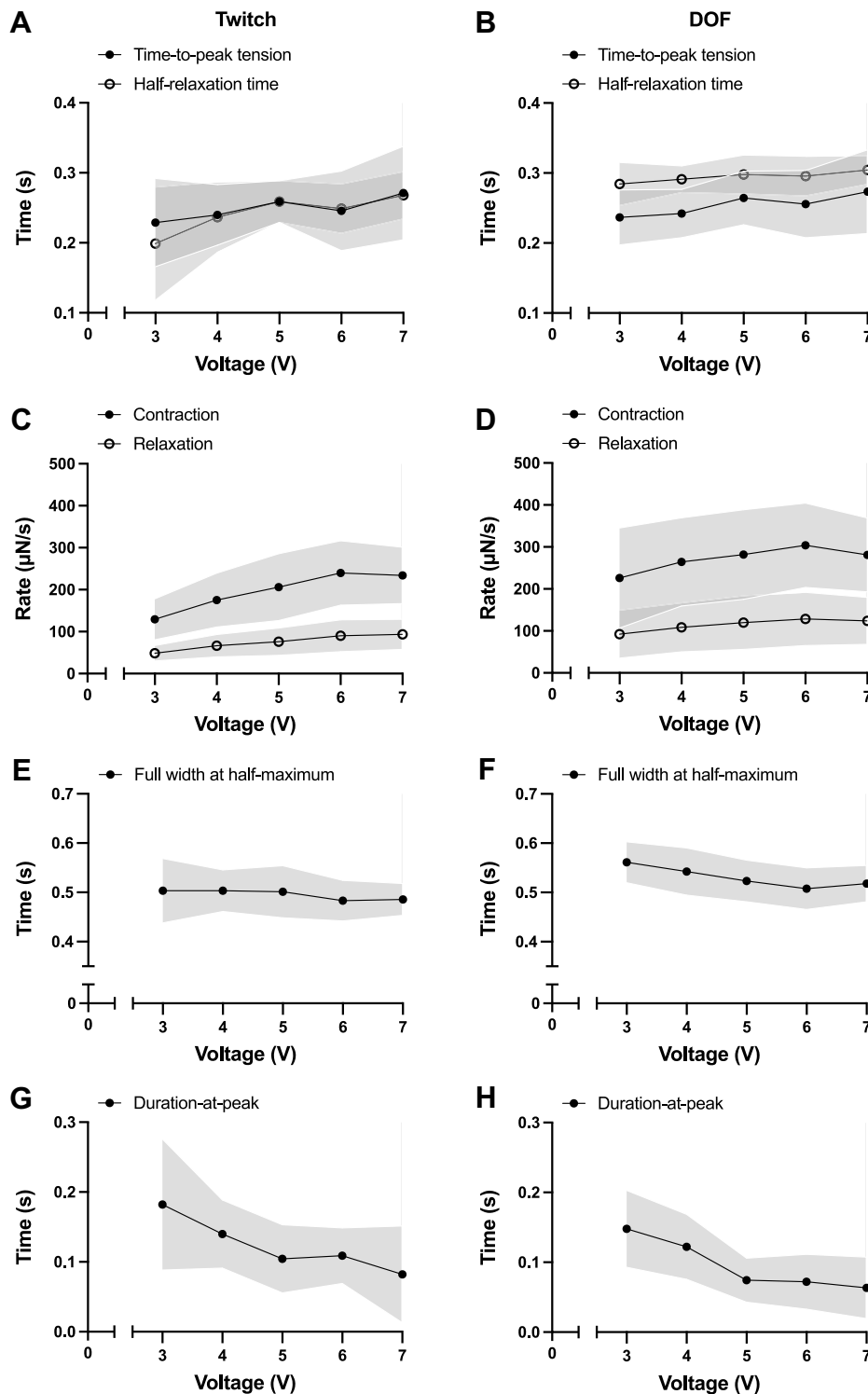


**Figure 4.** Peak twitch and dynamic oscillation of force (DOF) contraction kinetics at optimized pulse duration for 1 Hz stimulation. Kinetics of twitch (left; A, C, E, and G) and DOF (right; B, D, F, and H) contractions averaged across primary human skeletal muscle microtissues (hMMTs) cultured in MyoTACTIC from cell lines 1, 2, and 3. Pulse duration was 60 ms from 3 V to 7 V. Time-to-peak tension and half-relaxation time (A and B), contraction and relaxation rate (C and D), full-width at half-maximum (E and F), and duration-at-peak (G and H) were calculated. Summary data show means  $\pm$  SD (shaded regions) for  $n = 9$  hMMTs (with  $n = 3$  hMMTs from each cell line).

( $n = 3$  hMMTs), and  $247.4 \pm 32.7$   $\mu$ N ( $n = 3$  hMMTs), respectively (Supplemental Fig. S5). The difference in peak force between CL1 and CL3 was statistically significant ( $P = 0.002$ ; one-way ANOVA). Indeed, CL3 hMMTs produced the highest peak tetanic force, consistent with the results for peak twitch force. Microtissues derived from each myoblast line developed  $>85\%$  of peak force at 4 Hz, with modest increases in absolute force through 7 Hz then decreasing at higher

frequencies. The force developed by CL1 and CL2 hMMTs decreased gradually as stimulus frequency increased, whereas that elicited by CL3 hMMTs decreased sharply through 25 Hz and reached a plateau thereafter (Fig. 5B). In theory, temperature or fatigue could account for these differences, since we observed that prolonged time at room temperature (Supplemental Fig. S6A) and fatigue (Supplemental Fig. S6B) decreased hMMT force production. However, the

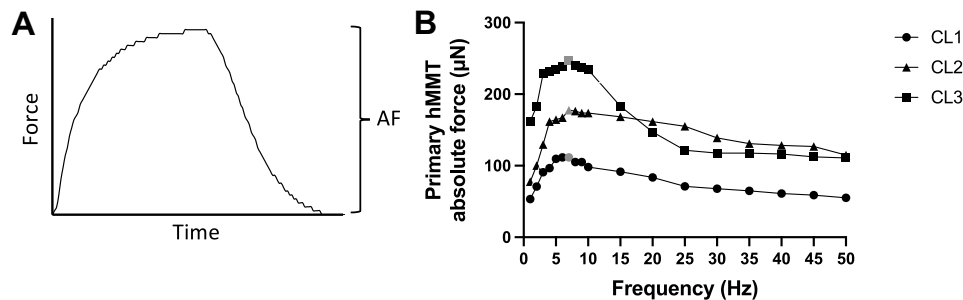


**Figure 5.** Optimization of stimulation frequency for peak tetanic force. **A:** graphical representation of absolute force (AF) derived from a representative fused tetanus force track elicited by primary human skeletal muscle microtissues (hMMTs) cultured in MyoTACTIC. **B:** absolute force produced by cell line 1 (CL1), cell line 2 (CL2), and cell line 3 (CL3) hMMTs at 5 V as frequency was increased from 1 Hz to 10 Hz in 1 Hz increments, and from 10 Hz to 50 Hz in 5 Hz increments. A pulse duration of 60 ms was used at 1 Hz stimulation frequency and reduced to pulse durations as low as 5 ms at higher frequencies to minimize tissue fatigue. Data show means of  $n = 3$ –5 hMMTs for each cell line.

rate in force loss attributable to these parameters accounts for a fraction of that observed with increasing frequency (Fig. 5B). Thus, evaluation of the frequency-force relationship revealed that although there are cell line-specific differences, peak tetanic force was elicited at 7 Hz, 5 V, and 10 ms for all hMMTs evaluated.

#### Peak Twitch Force of Immortalized hMMTs Is Elicited at 5 V, 80-ms Pulse Duration

To evaluate the generalizability of the EFS optimization protocol beyond primary hMMTs, we applied it to immortalized hMMTs cultured in the MyoTACTIC platform. In previous studies, we stimulated immortalized hMMTs at 0.5 Hz to assess twitch force (14, 28). Thus, to determine the optimal stimulus conditions for peak twitch tension, AB1167 immortalized hMMTs were stimulated at 0.5 Hz through a range of 1–10 V at pulse durations ranging from 5 ms to 80 ms (Fig. 6A). Higher voltage and longer pulse durations produced greater twitch force. Notably, voltages starting at 1 V were sufficient for hMMTs to generate micropost movement. Force peaked at 5 V, plateauing or decreasing thereafter, whereas electrolysis during EFS >5 V precluded force measurements beyond 7 V. As pulse duration was extended from 5 to 60 ms, incremental increases in force were observed, and a pronounced rise was observed at 80 ms.

The force tracks of immortalized and primary hMMTs revealed distinct contractile properties. Primary hMMTs underwent summation and required successive contractions in a 0.5 Hz stimuli train to stabilize force, thus necessitating the use of DOF to capture force trends (Fig. 2). In contrast, during repetitive stimulation at 0.5 Hz frequency, immortalized hMMTs returned to baseline between each stimulus, with the first contraction consistent with those to follow (Fig. 6B). Thus, twitch tension appropriately captured the force trends of immortalized hMMTs.

To evaluate the reproducibility of the EFS optimization protocol across micropost platforms, we applied it to hMMTs generated from AB1167 immortalized myoblasts in a custom PMMA micropost culture device. AB1167 immortalized hMMTs were stimulated at 0.5 Hz through a range of 1–10 V at pulse durations ranging from 5 ms to 100 ms (Fig. 6C). Consistent with findings in the MyoTACTIC platform, immortalized hMMTs did not exhibit summation during a 0.5 Hz stimuli train, and the first contraction in the train was

consistent with the ones that followed (Fig. 6D). Similarly, higher voltage and longer pulse produced greater twitch force. The absence of electrolysis during EFS in the PMMA platform enabled force measurements to be captured beyond 7 V, although the overall trends remain unchanged. Force peaked at 5 V, plateauing or decreasing at higher voltages. Incremental increases in force were observed as pulse duration was extended from 5 to 60 ms, rising from  $126.0 \pm 12.5 \mu\text{N}$  to  $188.8 \pm 29.2 \mu\text{N}$  at 5 V ( $n = 3$  hMMTs). At 80 ms, force exhibited a substantial increase, more than doubling at 5 V to  $398.2 \pm 140.3 \mu\text{N}$  ( $n = 3$  hMMTs). Beyond this, only a modest increase was observed at 100 ms, suggesting that the force elicited at 80 ms effectively represents the functional potential of immortalized hMMTs. In summary, peak twitch tension was consistently elicited at 5 V and 80 ms by immortalized hMMTs in both the MyoTACTIC and PMMA platforms. These studies demonstrate the generalizability of the protocol across cell lines, and the reproducibility of results across micropost platforms implemented by experimentalists at independent research institutions.

#### Peak Tetanic Force of Immortalized hMMTs Is Elicited at 35 Hz, 5 V, 10-ms Pulse Duration

We then applied the EFS optimization protocol to determine the frequency eliciting peak tetanic force from immortalized hMMTs cultured in the PMMA device. The force tracks of AB1167 hMMTs were measured from baseline to peak at stimulation frequencies ranging from 0.5 to 100 Hz, applying the optimal twitch electric field strength of 5 V (Fig. 6E). The absolute force generated by hMMTs increased steadily with rising stimulation frequency, reaching an average peak tetanic force of  $752.5 \pm 268.7 \mu\text{N}$  ( $n = 3$  hMMTs) at 35 Hz and a 10-ms pulse duration, before declining at higher frequencies. The frequency required to elicit peak tetanic force of immortalized hMMTs was five times higher than that for primary hMMTs, highlighting contractile property distinctions.

#### Peak Twitch Force of iPSC-Derived hMMTs Is Elicited at 5 V, 20-ms Pulse Duration

Human iPSC-derived myoblasts hold great potential in the field of skeletal muscle engineering, offering a renewable and patient-specific cell source for applications in transplantation and disease modeling (40). Therefore, we generated



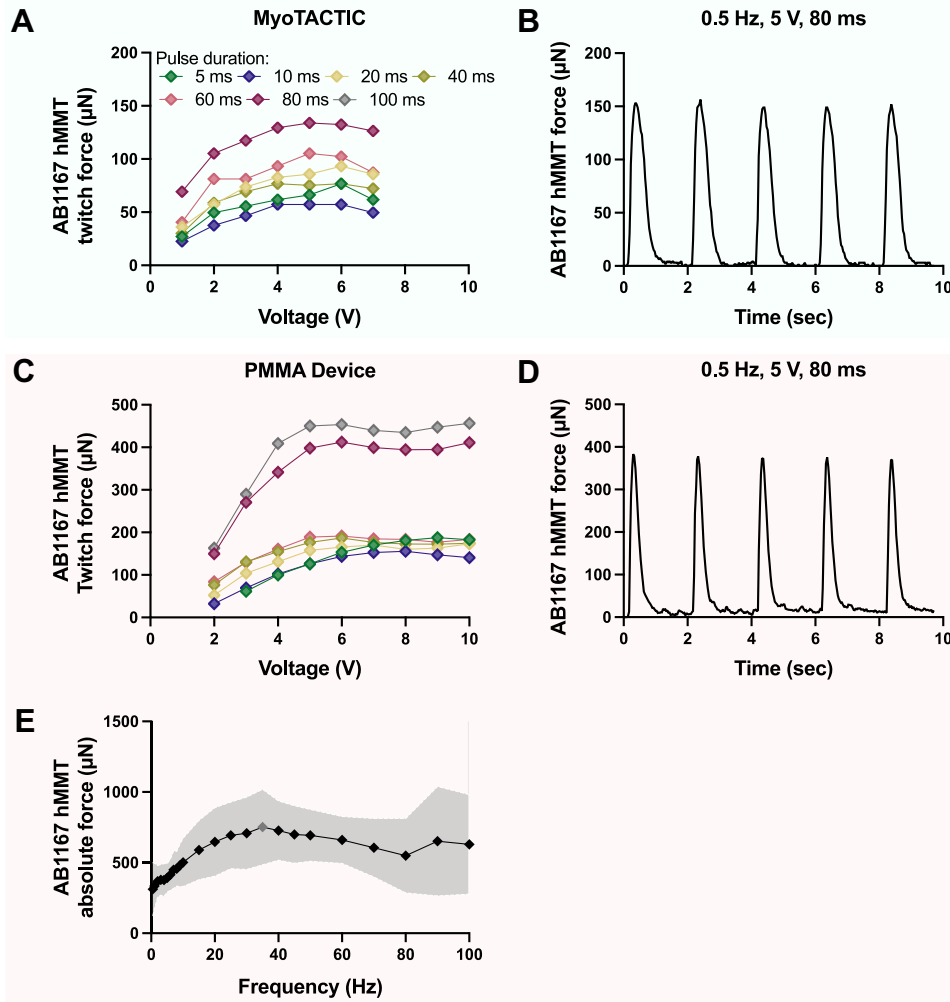


**Figure 6.** Application of the electrical field stimulation optimization protocol to immortalized human skeletal muscle microtissues. Twitch force produced by immortalized human skeletal muscle microtissues (hMMTs) at 0.5 Hz and pulse durations ranging from 5 ms up to 80 ms or 100 ms as voltage was increased by 1 V increments. hMMTs were generated from AB1167 myoblasts cultured in MyoTACTIC (A) and the polymethyl methacrylate (PMMA) (C) device. Data show mean values for  $n = 2$  hMMTs in (A) and  $n = 3$  hMMTs in (C). Representative force tracks elicited at peak twitch electrical field stimulation (EFS) parameters by AB1167 hMMTs cultured in MyoTACTIC (B) and the PMMA (D) device. E: absolute force produced by AB1167 hMMTs cultured in the PMMA device at 5 V as frequency was increased from 0.5 Hz to 100 Hz. A pulse duration of 80 ms was used at 0.5 Hz stimulation frequency and reduced to pulse durations as low as 10 ms at higher frequencies to minimize tissue fatigue. Data show means  $\pm$  SD (shaded region) for  $n = 3$  hMMTs. MyoTACTIC and PMMA hMMT data panels are shaded in blue and pink, respectively.

myoblasts from a human iPSC line, produced hMMTs in the PMMA device, and applied the EFS protocol to identify the optimal stimulus conditions eliciting peak twitch force from iPSC-derived hMMTs. hMMTs were stimulated at 1 Hz through a range of 1–10 V at pulse durations ranging from 5 ms to 80 ms. Twitch force (Fig. 7A) and DOF (Fig. 7B) values were measured from the force tracks. Force increased with voltage, peaking at 6 V for twitch force and 5 V for DOF, and decreased thereafter. The decline in DOF was particularly pronounced, dropping to  $\sim 20\%$ – $35\%$  of peak by 10 V for select stimulus durations. This reduction is attributable to iPSC-derived hMMTs undergoing summation at EFS  $> 5$  V (Fig. 7C), which identified 5 V as the optimal electric field strength. Notably, DOF for EFS at 60 ms and 80 ms is not reported at voltages  $> 5$  V due to the onset of summation that obscured the resolution of DOF. With respect to pulse duration, slight increases in force were observed with longer durations, reaching a maximum at 20 ms and subsequently decreasing. Thus, iPSC-derived hMMTs cultured in the PMMA device elicit peak twitch tension at 5 V and 20 ms. The successful application of the EFS optimization protocol to iPSC-derived hMMTs further demonstrates its utility across cell lines and micropost platforms, while revealing contractile properties unique to hMMTs generated from iPSC-derived

myoblasts. The twitch kinetics of immortalized AB1167 and iPSC-derived hMMTs at the EFS parameters eliciting peak twitch force are provided in Supplemental Table S4.

### Peak Tetanic Force of iPSC-Derived hMMTs Is Elicited at 60 Hz Frequency, 5 V, 10-ms Pulse Duration

The EFS optimization protocol was applied to determine the frequency eliciting peak tetanic force from iPSC-derived hMMTs cultured in the PMMA device. The force tracks of iPSC-derived hMMTs were measured from baseline to peak at stimulation frequencies ranging from 1 to 100 Hz, applying the optimal twitch electric field strength of 5 V (Fig. 7D). The absolute force generated by hMMTs increased incrementally with rising stimulation frequency, reaching an average peak tetanic force of  $232.9 \pm 33.2 \mu\text{N}$  ( $n = 3$  hMMTs) at 60 Hz and a 10-ms pulse duration. Unlike primary and immortalized hMMTs, iPSC-derived hMMTs did not exhibit a decline in force at higher stimulation frequencies.

## DISCUSSION

We present a systematic optimization protocol to establish the EFS parameters eliciting peak twitch and tetanus force from muscle microtissues. These parameters measure the

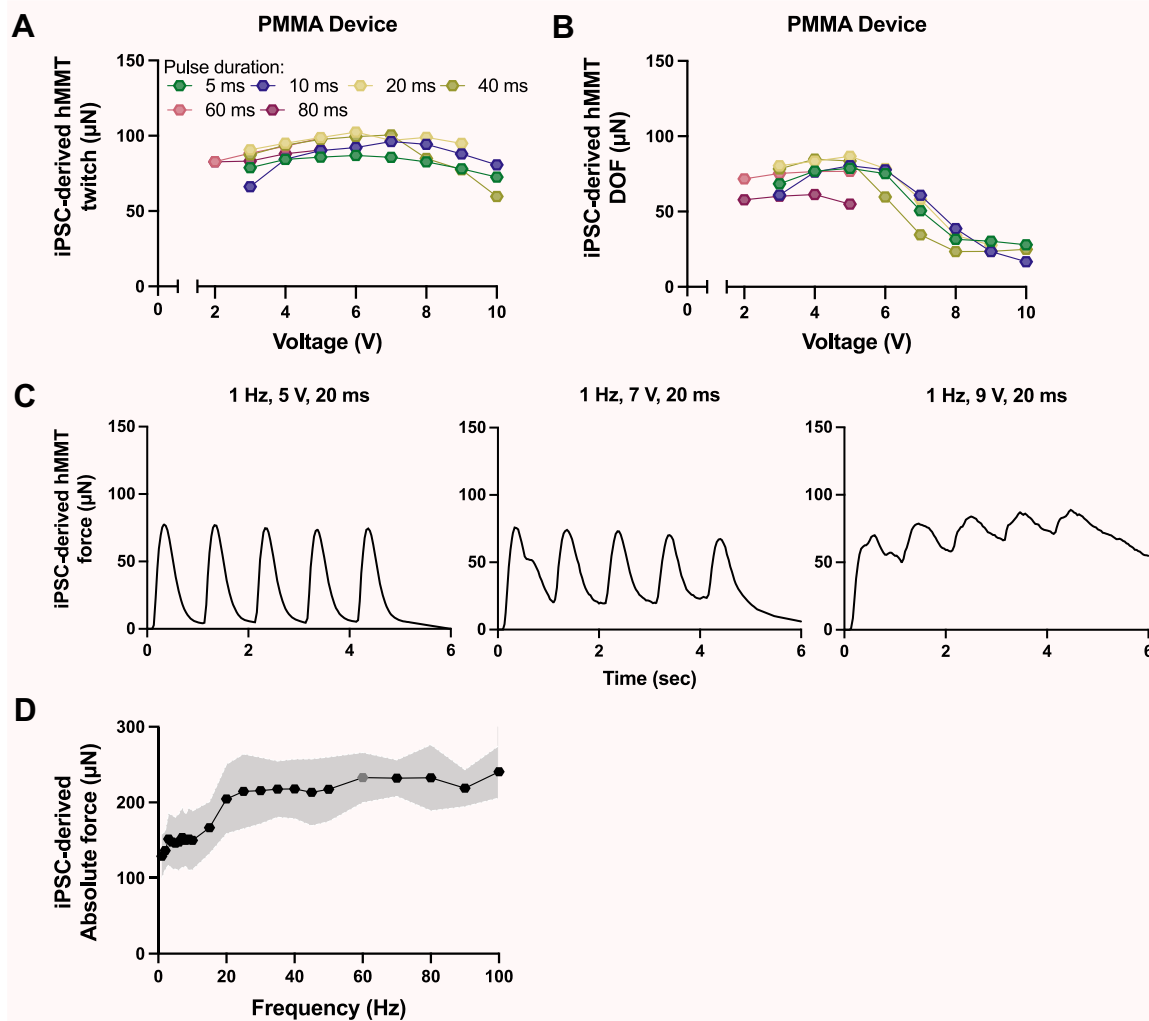


**Figure 7.** Application of the electrical field stimulation optimization protocol to induced pluripotent stem cell (iPSC)-derived human skeletal muscle microtissues (hMMTs). The twitch force (A) and dynamic oscillation of force (DOF, B) produced by iPSC-derived hMMTs cultured in the polymethyl methacrylate (PMMA) device at 1 Hz and pulse duration ranging from 5 ms to 80 ms as voltage was increased by 1 V increments. Data show mean values for  $n = 2$  or 3 hMMTs in each panel. C: representative force tracks elicited by the peak twitch stimulation duration of 20 ms at 5 V, 7 V, and 9 V. D: absolute force produced by iPSC-derived hMMTs cultured in the PMMA device at 5 V as frequency was increased from 1 Hz to 100 Hz. A pulse duration of 20 ms was used at 1 Hz stimulation frequency and reduced to pulse durations as low as 10 ms at higher frequencies to minimize tissue fatigue. Data show means  $\pm$  SD (shaded region) for  $n = 3$  hMMTs. Pink shading indicates that figure panels correspond to PMMA hMMT data.

true functional potential of microtissues in micropost devices that are otherwise masked by inappropriate EFS parameters. Optimized EFS parameters were determined to assess the contractile function of primary, immortalized, and iPSC-derived hMMTs cultured in the MyoTACTIC and PMMA micropost deflection platforms. Peak twitch force was elicited with stimulus durations of 20–80 ms, and peak tetanic force was achieved at stimulation frequencies of 7–60 Hz, both using an electric field strength of 5 V. The range of the optimized EFS parameters highlights cell line-type specific differences, emphasizing the need for optimization, while demonstrating the protocol's usability by researchers at different institutions and broad applicability across cell lines and micropost deflection platforms. This systematic optimization also uncovered shortcomings of using the twitch as a metric to assess the contractile properties of primary hMMTs, underestimating force production and contraction

kinetics in response to a single stimulus. To address these shortcomings, we propose a companion metric for twitch force, the dynamic oscillation of force (DOF), which defines the difference between minimal and peak force during stabilized rhythmic contractions at 1 Hz. We also extend the kinetics parameters to include duration-at-peak force for primary microtissues. Our findings provide a framework based on the contractile properties of native skeletal muscle that is adapted to those of engineered muscle constructs. These data can guide those who engineer muscle constructs in defining optimal EFS parameters and their presentation of functional outcomes.

Electrical field stimulation is used to evaluate the contractile properties of isolated native muscles for studies *in vitro* (26, 36) and for evaluating native muscle function *in situ* (41). Stimulation of native muscle in these applications with pulse durations of 0.1–1 ms is sufficient to elicit peak

twitch and tetanic force. In comparison, a pulse duration of 0.1 ms was not sufficient to produce micropost movement in hMMTs. In theory, this limitation may be resolved by fabricating more flexible microposts, but in practice, this design change does not offer the axial tension required to support engineered muscle tissue development. Longer depolarizations of the sarcolemma were required to initiate excitation-contraction coupling in our muscle microtissues, with peak force produced at 20–80 ms pulse durations in an electrical field of 5 V (Figs. 1, 3, 6, and 7). Microtissues generated from primary, immortalized, and iPSC-derived myoblasts exhibited differences in the pulse durations required to achieve peak twitch force. However, immortalized microtissues cultured in both the MyoTACTIC and PMMA platforms produced peak twitch force at the same pulse duration, suggesting that the differences observed are cell-type specific rather than platform dependent.

In addition to requiring longer depolarization of the sarcolemma, hMMTs also displayed slower contraction kinetics than native muscle. The time-to-peak tension and half-time relaxation time values for primary hMMT twitch contractions (Fig. 4A) were ~24% and ~100% longer, respectively, than those measured for adult human skeletal muscle at 24°C *in situ* (42). A comparison to EFS of native adult skeletal muscle at 24°C is reasonable given that temperature in the range of 24°C–26°C was recorded for media in the well prior and following hMMT stimulation. In addition to longer contraction and relaxation times, we observed prolongation of peak tension for primary hMMT twitch contractions, specific to engineered skeletal muscle, which we quantified as the duration-at-peak. When stimulated at 37°C, microtissues continued to display slower contraction kinetics compared with native muscle. For example, the time-to-peak tension and half-time relaxation time values for immortalized AB1167 hMMTs cultured in the PMMA device (Supplemental Table S4) were 97% and 124% longer, respectively, than those measured for adult human skeletal muscle at 37°C *in situ* (42). Slower contraction kinetics were observed across all cell lines and micropost platforms assessed. A systematic comparison of EFS at RT and 37°C is needed to determine whether stimulation at lower temperatures exacerbates the difference in contraction kinetics between engineered and native skeletal muscle.

The need to stimulate with longer pulse durations to elicit detectable contraction, and the slower contraction kinetics of hMMTs, implies poor excitation-contraction coupling and underdeveloped calcium handling. This is in line with the finding of a presumptive SR and T-tubule profile, but no triads, in 3-D skeletal muscle microtissues generated from immortalized cells (43). To develop triad structures in this muscle model, cocultures with iPSC-derived motor neurons were required. In addition, although 3-D cultures have more mature protein expression than myotubes cultured in 2-D (44), there is a dominance of fetal proteins (e.g., embryonic myosin heavy chain isoforms) over adult skeletal muscle sarcomeric and calcium handling proteins in primary 3-D cultures as compared with native skeletal muscle (45). Despite these differences, engineered skeletal muscle remains a robust platform to compare contractile function under control versus diseased conditions. Furthermore, the protocol reported herein offers a valuable approach to evaluate methodologies

aimed at enhancing the contractile properties of engineered muscle, with the goal of bringing it closer to the form and function of native tissue.

The variation in stimulation frequencies required to elicit peak tetanic force among microtissues further demonstrates the cell-type specific differences in contractile function of hMMTs. The measure of force as a function of stimulation frequency produces a sigmoidal curve that plateaus at 20–50 Hz in native adult skeletal muscle (46–48). Primary hMMTs displayed a shift to lower frequencies, producing a peak in force at 7 Hz (Fig. 5B). This may be due to the slower release and removal of calcium to initiate and terminate force production, respectively. As more time is required for the contraction and relaxation phases, primary hMMTs are prone to summation, therefore, fused tetanus is elicited at lower frequencies. In contrast, immortalized hMMTs produced peak tetanic force at 35 Hz (Fig. 6E), within the 20–50 Hz range typical of native human skeletal muscle, likely reflecting their faster contraction kinetics. Following the peak force observed at 7 Hz for primary hMMTs (Fig. 5B) and 35 Hz for immortalized hMMTs (Fig. 6E), a sharp decline in force was evident for both cell types. For primary hMMTs, a portion of this reduction can be partially attributed to extended time at room temperature and fatigue from repetitive contractions accounts (Supplemental Fig. S6). Repeated high-frequency stimulation may also compromise the calcium-handling and contractile machinery. For iPSC-derived hMMTs, the highest stimulation frequency, 60 Hz, was required to produce peak tetanic force. Although iPSC-derived hMMTs undergo fused tetanus at lower frequencies similar to primary hMMTs, the need for higher stimulation frequencies may reflect a greater threshold to achieve the intracellular calcium concentration necessary for maximal force generation by the contractile proteins.

During a 1-Hz stimulation train, iPSC-derived hMMTs exhibited summation only when an electric field of >5 V was applied (Fig. 7), supporting the selection of 5 V as the optimal twitch electric field strength. Conversely, primary hMMTs exhibited summation at all tested voltages during repetitive 1 Hz stimulation (Fig. 3). To better quantify these contractions, we introduced the metric DOF as the difference in minimal and peak force in a train of 1 Hz stimuli. This differs from the standard measure of force that is based on a single twitch or tetanic contraction from the muscle's resting state. DOF thereby provides a dynamic index of hMMT contractions.

The contraction kinetics of microtissues in flexible micropost models differ from those expected under isometric conditions. In micropost platforms, the post displacement generated by a microtissue during contraction is proportional to the exerted force. However, depending on the elasticity of the posts, the tension within the microtissue may return to baseline faster than the posts return to their resting state. As a result, the summation observed during EFS of primary hMMTs at 1 Hz could be an artifact of PDMS micropost pliancy. Nonetheless, this does not negate the observation that summation occurred during contractions of primary hMMTs but not those of immortalized hMMTs, which were cultivated in PDMS and PMMA devices. Thus, the differential contractile properties of the microtissues are not masked by potential platform-related artifacts, enabling a reliable comparison of microtissue contractile behavior under varying experimental conditions.



In the process of optimizing the electrical stimulation parameters for hMMTs, we resolved the decline of primary hMMT contractile function at RT, which is likely a property shared by all engineered skeletal muscle constructs. For *ex vivo* studies of rat skeletal muscle, tissue integrity and contractile function are affected by temperature. Isolated soleus and extensor digitorum longus muscles developed a larger hypoxic core and were quicker to fatigue at incubation temperatures above 25°C and 30°C, respectively (26, 36). Thus, to increase the stability and minimize fatigue, we initially equilibrated hMMTs at 25°C before performing electrical stimulation at RT. However, we found that hMMT contractile force decreased over time (Supplemental Figs. S1, S3, and S6A). Thus, we adopted the procedure of stimulating hMMTs cultured in MyoTACTIC directly following removal from the incubator. Although temperature in the well was 24°C–26°C when EFS was performed, rewarming between each microtissue in a multiwell plate minimized the time hMMTs were at RT. Although immortalized hMMTs cultured in MyoTACTIC were stimulated at RT, EFS for those cultured in the PMMA device was conducted within a temperature-controlled cage incubator at 37°C. The difference in study temperature may explain distinctions in absolute force generated for AB1167 hMMTs across the two platforms, though the twofold difference in cell seeding density across the two devices is an alternative explanation. Despite this variation in experimental conditions, identical optimized EFS twitch parameters were identified. This outcome demonstrates the reproducibility of the optimization protocol's applicability across micropost deflection platforms and indicates that stimulation at RT does not compromise trends within an experiment that are revealed by the protocol.

The consistent differences in strength between hMMTs from different primary cell lines suggest that the source of myoblasts affects the contractile function of microtissues. CL3 hMMTs generated from the muscle biopsy of an active 18-yr-old male were consistently stronger than CL2 and CL1 hMMTs from the biopsies of a 19-yr-old female and 64-yr-old male, respectively (Supplemental Figs. S2, S4, and S5). There is evidence that some properties of the donor muscle *in vivo* are maintained *in vitro*. For example, defects in the glucose and lipid metabolism of myotubes from individuals with diabetes have been demonstrated, as compared with those from obese or lean donors (49). Such differences provide an opportunity to model and investigate disease states, but also emphasize the importance of selecting appropriate inclusion and exclusion criteria for donors in studies of engineered muscle.

To conclude, we report a protocol for optimizing the electrical stimulation parameters for peak twitch and peak tetanus force, and introduce DOF and duration-at-peak as new analysis parameters to evaluate engineered muscle tissues. Our work highlights that the optimal EFS and temperature conditions established for the functional characterization of native skeletal muscle may not always be suitable to microtissues. Rather, the EFS parameters for hMMTs derived from different cell line types must be individually tailored, as a universal set of parameters is not applicable with the currently available methods for generating engineered muscle tissues. Indeed, studies reporting force produced by treated or diseased tissues, relative to a control, would similarly benefit from

optimizing EFS parameters to define the range through which significant differences in force production can be detected. Optimizing and reporting EFS parameters, and applying appropriate metrics for the evaluation of contractile function, will promote the use of muscle microtissues in biomedical research. Based on the present data showing delayed kinetics, a key goal is to develop the excitation-contraction coupling system to more closely approximate that of native muscle.

## DATA AVAILABILITY

The datasets generated during and analyzed in this study are available from the corresponding author on reasonable request.

## SUPPLEMENTAL MATERIAL

Supplemental Figs. S1–S6: <https://doi.org/10.6084/m9.figshare.28365566>.

Supplemental Tables S1–S4: <https://doi.org/10.6084/m9.figshare.28365590>.

## ACKNOWLEDGMENTS

Schematics were produced using BioRender. We also extend our gratitude to ArtifiCell GmbH for generously providing PMMA devices for the fabrication of immortalized and iPSC-derived hMMTs used in these studies.

## GRANTS

This project was funded by a Canada First Research Excellence Fund “Medicine by Design (MbD)” grant (to P.M.G.) Y.T. was supported by a Barbara Frank and Milligan Award and a Wildcat Graduate Scholarship. H.L. was supported by an Ontario Graduate Scholarship, Cecil Yip Doctoral Research Award, a Wildcat Graduate Scholarship, and the Faculty of Applied Science and Engineering Student Endowment Fund (APSC GSEF) Award. T.B. was funded by the Deutsche Forschungsgemeinschaft (DFG, German Research Foundation) under Grant Nos. 450595133 and 456112451. W.-H.Z. was supported by the German Centre for Cardiovascular Research (DZHK), the German Federal Ministry of Science and Education under Grant No. BMBF FKZ 161L0250A, the German Research Foundation under Grant No. EXC 2067-1, and the Leducq Foundation under Grant No. 20CVD04. S.S.S. was supported by National Institutes of Health Grant 1R21HD110771-01A1. P.M.G. was supported by a Canada Research Chair in Endogenous Repair under Award No. 950-231201.

## DISCLOSURES

A.H., T.B., and M.L. are scientists and cofounders at ArtifiCell GmbH. W.-H.Z. is founder, equity holder, and advisor of Repairon GmbH and myriamed GmbH. None of the other authors has any conflicts of interest, financial or otherwise, to disclose.

## AUTHOR CONTRIBUTIONS

Y.T., A.B.M., S.S.S., and P.M.G. conceived and designed research; Y.T., Z.X., A.H., R.K., and H.L. performed experiments; Y.T., Z.X., H.L., and A.H. analyzed data; Y.T., A.B.M., S.S.S., and P.M.G. interpreted results of experiments; Y.T. and Z.X. prepared figures; Y.T. and P.M.G. drafted manuscript; Y.T., Z.X., A.H., H.L., M.L., R.K., T.B., W.-H.Z., A.B.M., S.S.S., and P.M.G. edited and revised manuscript; Y.T., Z.X., A.H., H.L., M.L., R.K., T.B., W.-H.Z., A.B.M., S.S.S., and P.M.G. approved final version of manuscript.

## REFERENCES

- Mukund K, Subramaniam S. Skeletal muscle: a review of molecular structure and function, in health and disease. *Wiley Interdiscip Rev Syst Biol Med* 12: e1462, 2020. doi:10.1002/wsbm.1462.
- Hoffmann C, Weigert C. Skeletal muscle as an endocrine organ: the role of myokines in exercise adaptations. *Cold Spring Harb Perspect Med* 7: a029793, 2017. doi:10.1101/cshperspect.a029793.
- Bolaños P, Calderón JC. Excitation-contraction coupling in mammalian skeletal muscle: Blending old and last-decade research. *Front Physiol* 13: 989796, 2022. doi:10.3389/fphys.2022.989796.
- Butterfield RJ. Congenital muscular dystrophy and congenital myopathy. *Continuum (Minneapolis)* 25: 1640–1661, 2019. doi:10.1212/CON.0000000000000792.
- Tidball JG. Mechanisms of muscle injury, repair, and regeneration. *Compr Physiol* 1: 2029–2062, 2011. doi:10.1002/cphy.c100092.
- Morton AB, Norton CE, Jacobsen NL, Fernando CA, Cornelison DDW, Segal SS. Barium chloride injures myofibers through calcium-induced proteolysis with fragmentation of motor nerves and microvessels. *Skelet Muscle* 9: 27, 2019. doi:10.1186/s13395-019-0213-2.
- Dao T, Green AE, Kim YA, Bae S-J, Ha K-T, Gariani K, Lee M, Menzies KJ, Ryu D. Sarcopenia and muscle aging: a brief overview. *Endocrinol Metab (Seoul)* 35: 716–732, 2020. doi:10.3803/EnM.2020.405.
- Yucel N, Chang AC, Day JW, Rosenthal N, Blau HM. Humanizing the mdx mouse model of DMD: the long and the short of it. *NPJ Regen Med* 3: 4, 2018 [Erratum in *NPJ Regen Med* 5: 25, 2020]. doi:10.1038/s41536-018-0045-4.
- Afzali AM, Ruck T, Wiendl H, Meuth SG. Animal models in idiopathic inflammatory myopathies: How to overcome a translational roadblock? *Autoimmun Rev* 16: 478–494, 2017. doi:10.1016/j.autrev.2017.03.001.
- Shen H-W, Jiang X-L, Gonzalez FJ, Yu A-M. Humanized transgenic mouse models for drug metabolism and pharmacokinetic research. *Curr Drug Metab* 12: 997–1006, 2011. doi:10.2174/138920011798062265.
- Guo X, Greene K, Akanda N, Smith AST, Stancescu M, Lambert S, Vandeburgh H, Hickman JJ. In vitro differentiation of functional human skeletal myotubes in a defined system. *Biomater Sci* 2: 131–138, 2014. doi:10.1039/C3BM60166H.
- Brunetti J, Koenig S, Monnier A, Frieden M. Nanopattern surface improves cultured human myotube maturation. *Skelet Muscle* 11: 12, 2021. doi:10.1186/s13395-021-00268-3.
- Cooper ST, Maxwell AL, Kizana E, Ghodousi M, Hardeman EC, Alexander IE, Allen DG, North KN. C2C12 co-culture on a fibroblast substratum enables sustained survival of contractile, highly differentiated myotubes with peripheral nuclei and adult fast myosin expression. *Cell Motil Cytoskeleton* 58: 200–211, 2004. doi:10.1002/cm.20010.
- Ebrahimi M, Lad H, Fusto A, Tiper Y, Datye A, Nguyen CT, Jacques E, Moyle LA, Nguyen T, Musgrave B, Chávez-Madero C, Bigot A, Chen C, Turner S, Stewart BA, Pegoraro E, Vitiello L, Gilbert PM. De novo revertant fiber formation and therapy testing in a 3D culture model of Duchenne muscular dystrophy skeletal muscle. *Acta Biomater* 132: 227–244, 2021. doi:10.1016/j.actbio.2021.05.020.
- Badu-Mensah A, Guo X, McAleer CW, Rumsey JW, Hickman JJ. Functional skeletal muscle model derived from SOD1-mutant ALS patient iPSCs recapitulates hallmarks of disease progression. *Sci Rep* 10: 14302, 2020. doi:10.1038/s41598-020-70510-3.
- Shimizu K, Genma R, Gotou Y, Nagasaka S, Honda H. Three-dimensional culture model of skeletal muscle tissue with atrophy induced by dexamethasone. *Bioengineering (Basel)* 4: 56, 2017. doi:10.3390/bioengineering4020056.
- Afshar ME, Abrahama HY, Bakoosli MA, Davoudi S, Thavandiran N, Tung K, Ahn H, Ginsberg HJ, Zandstra PW, Gilbert PM. A 96-well culture platform enables longitudinal analyses of engineered human skeletal muscle microtissue strength. *Sci Rep* 10: 6918, 2020. doi:10.1038/s41598-020-62837-8.
- Madden L, Juhas M, Kraus WE, Truskey GA, Bursac N. Bioengineered human myobundles mimic clinical responses of skeletal muscle to drugs. *eLife* 4: e04885, 2015. doi:10.7554/eLife.04885.
- Ikeda K, Ito A, Imada R, Sato M, Kawabe Y, Kamihira M. In vitro drug testing based on contractile activity of C2C12 cells in an epigenetic drug model. *Sci Rep* 7: 44570, 2017. doi:10.1038/srep44570.
- Vesga-Castro C, Aldazabal J, Vallejo-Illarramendi A, Paredes J. Contractile force assessment methods for in vitro skeletal muscle tissues. *eLife* 11: e77204, 2022. doi:10.7554/eLife.77204.
- Smith AST, Long CJ, Pirozzi K, Najjar S, McAleer C, Vandeburgh HH, Hickman JJ. A multiplexed chip-based assay system for investigating the functional development of human skeletal myotubes in vitro. *J Biotechnol* 185: 15–18, 2014. doi:10.1016/j.jbiotec.2014.05.029.
- Santoso JW, Li X, Gupta D, Suh GC, Hendricks E, Lin S, Perry S, Ichida JK, Dickman D, McCain ML. Engineering skeletal muscle tissues with advanced maturity improves synapse formation with human induced pluripotent stem cell-derived motor neurons. *APL Bioeng* 5: 036101, 2021. doi:10.1063/5.0054984.
- Hofemeier AD, Limon T, Muenker TM, Wallmeyer B, Jurado A, Afshar ME, Ebrahimi M, Tsukanov R, Oleksievets N, Enderlein J, Gilbert PM, Betz T. Global and local tension measurements in biomimetic skeletal muscle tissues reveals early mechanical homeostasis. *eLife* 10: e60145, 2021. doi:10.7554/eLife.60145.
- Vandeburgh H, Shansky J, Benesch-Lee F, Barbata V, Reid J, Thorrez L, Valentini R, Crawford G. Drug-screening platform based on the contractility of tissue-engineered muscle. *Muscle Nerve* 37: 438–447, 2008. doi:10.1002/mus.20931.
- Wang K, Smith SH, Iijima H, Hettinger ZR, Mallepally A, Shroff SG, Ambrosio F. Bioengineered 3D skeletal muscle model reveals complement 4b as a cell-autonomous mechanism of impaired regeneration with aging. *Adv Mater* 35: e2207443, 2023. doi:10.1002/adma.202207443.
- Segal SS, Faulkner JA, White TP. Skeletal muscle fatigue in vitro is temperature dependent. *J Appl Physiol* (1985) 61: 660–665, 1986. doi:10.1152/jappl.1986.61.2.660.
- Khodabakus A, Baar K. Defined electrical stimulation emphasizing excitability for the development and testing of engineered skeletal muscle. *Tissue Eng Part C Methods* 18: 349–357, 2012. doi:10.1089/ten.tec.2011.0364.
- Lad H, Musgrave B, Ebrahimi M, Gilbert PM. Assessing functional metrics of skeletal muscle health in human skeletal muscle microtissues. *J Vis Exp* e62307, 2021. doi:10.3791/62307.
- Zhang H, Chiao M. Anti-fouling coatings of poly(dimethylsiloxane) devices for biological and biomedical applications. *J Med Biol Eng* 35: 143–155, 2015. doi:10.1007/s40846-015-0029-4.
- Blau HM, Webster C. Isolation and characterization of human muscle cells. *Proc Natl Acad Sci U S A* 78: 5623–5627, 1981. doi:10.1073/pnas.78.9.5623.
- Baghbaderani BA, Tian X, Neo BH, Burkall A, Dimezzo T, Sierra G, Zeng X, Warren K, Kovarcik DP, Fellner T, Rao MS. CGMP-manufactured human induced pluripotent stem cells are available for pre-clinical and clinical applications. *Stem Cell Reports* 5: 647–659, 2015. doi:10.1016/j.stemcr.2015.08.015.
- Shahriyari M, Islam MR, Sakib SM, Rinn M, Rika A, Krüger D, Kaurani L, Gisa V, Winterhoff M, Anandakumar H, Shomroni O, Schmidt M, Salinas G, Unger A, Linke WA, Zschüntzsch J, Schmidt J, Bassel-Duby R, Olson EN, Fischer A, Zimmermann WH, Tiburcy M. Engineered skeletal muscle recapitulates human muscle development, regeneration and dystrophy. *J Cachexia Sarcopenia Muscle* 13: 3106–3121, 2022. doi:10.1002/jcsm.13094.
- Shahriyari M, Rinn M, Hofemeier AD, Babych A, Zimmermann WH, Tiburcy M. Protocol to develop force-generating human skeletal muscle organoids. *STAR Protoc* 5: 102794, 2024. doi:10.1016/j.xpro.2023.102794.
- Munker T. Electric Stimulation Software. 2023. <https://github.com/Tillmuen09/ElectricStimulationSoftware>.
- Gilbert Lab. MyoTACTIC. 2024. <https://github.com/gilbertlabcode/myoTACTIC>.
- Segal SS, Faulkner JA. Temperature-dependent physiological stability of rat skeletal muscle in vitro. *Am J Physiol* 248: C265–C270, 1985. doi:10.1152/ajpcell.1985.248.3.C265.
- Bigland-Ritchie B, Thomas CK, Rice CL, Howarth JV, Woods JJ. Muscle temperature, contractile speed, and motoneuron firing rates during human voluntary contractions. *J Appl Physiol* (1985) 73: 2457–2461, 1992. doi:10.1152/jappl.1992.73.6.2457.
- Han R, Bakker AJ. The effect of chelerythrine on depolarization-induced force responses in skinned fast skeletal muscle fibres of the rat. *Br J Pharmacol* 138: 417–426, 2003. doi:10.1038/sj.bjp.0705035.

39. **Kesar T, Chou LW, Binder-Macleod SA.** Effects of stimulation frequency versus pulse duration modulation on muscle fatigue. *J Electromyogr Kinesiol* 18: 662–671, 2008. doi:[10.1016/j.jelekin.2007.01.001](https://doi.org/10.1016/j.jelekin.2007.01.001).
40. **Moyle LA, Jacques E, Gilbert PM.** Engineering the next generation of human skeletal muscle models: From cellular complexity to disease modeling. *Curr Opin Biomed Eng* 16: 9–18, 2020. doi:[10.1016/j.cobme.2020.05.006](https://doi.org/10.1016/j.cobme.2020.05.006).
41. **Manabe Y, Fujii NL.** Experimental research models for skeletal muscle contraction. *J Phys Fitness Sports Med* 5: 373–377, 2016. doi:[10.7600/jpfs.5.373](https://doi.org/10.7600/jpfs.5.373).
42. **Davies CTM, Mecrow IK, White MJ.** Contractile properties of the human triceps surae with some observations on the effects of temperature and exercise. *Eur J Appl Physiol Occup Physiol* 49: 255–269, 1982. doi:[10.1007/BF02334074](https://doi.org/10.1007/BF02334074).
43. **Nguyen CT, Chávez-Madero C, Jacques E, Musgrave B, Yin T, Saraci K, Gilbert PM, Stewart BA, Stewart B.** Electron microscopic analysis of the influence of iPSC-derived motor neurons on bioengineered human skeletal muscle tissues. *Cell Tissue Res* 396: 57–69, 2024. doi:[10.1007/s00441-024-03864-z](https://doi.org/10.1007/s00441-024-03864-z).
44. **Rao L, Qian Y, Khodabukus A, Ribar T, Bursac N.** Engineering human pluripotent stem cells into a functional skeletal muscle tissue. *Nat Commun* 9: 126, 2018. doi:[10.1038/s41467-017-02636-4](https://doi.org/10.1038/s41467-017-02636-4).
45. **Mills RJ, Parker BL, Monnot P, Needham EJ, Vivien CJ, Ferguson C, Parton RG, James DE, Porrello ER, Hudson JE.** Development of a human skeletal micro muscle platform with pacing capabilities. *Biomaterials* 198: 217–227, 2019. doi:[10.1016/j.biomaterials.2018.11.030](https://doi.org/10.1016/j.biomaterials.2018.11.030).
46. **Yan S, Gauthier AP, Similowski T, Faltus R, Macklem PT, Bellemare F.** Force-frequency relationships of in vivo human and in vitro rat diaphragm using paired stimuli. *Eur Respir J* 6: 211–218, 1993. doi:[10.1183/09031936.93.06020211](https://doi.org/10.1183/09031936.93.06020211).
47. **Binder-Macleod SA, Lee SC, Fritz AD, Kucharski LJ.** New look at force-frequency relationship of human skeletal muscle: effects of fatigue. *J Neurophysiol* 79: 1858–1868, 1998. doi:[10.1152/jn.1998.79.4.1858](https://doi.org/10.1152/jn.1998.79.4.1858).
48. **Orizio C, Gobbo M, Diemont B.** Changes of the force-frequency relationship in human tibialis anterior at fatigue. *J Electromyogr Kinesiol* 14: 523–530, 2004. doi:[10.1016/j.jelekin.2004.03.009](https://doi.org/10.1016/j.jelekin.2004.03.009).
49. **Aas V, Bakke SS, Feng YZ, Kase ET, Jensen J, Bajpeyi S, Thoresen GH, Rustan AC.** Are cultured human myotubes far from home? *Cell Tissue Res* 354: 671–682, 2013. doi:[10.1007/s00441-013-1655-1](https://doi.org/10.1007/s00441-013-1655-1).